A NOVEL STAPHYLOCOCCUS AUREUS-MODIFIED ELECTROCHEMICAL BIOSENSOR FOR DETERMINATION OF HEAVY METALS

by

Parsa Pishva
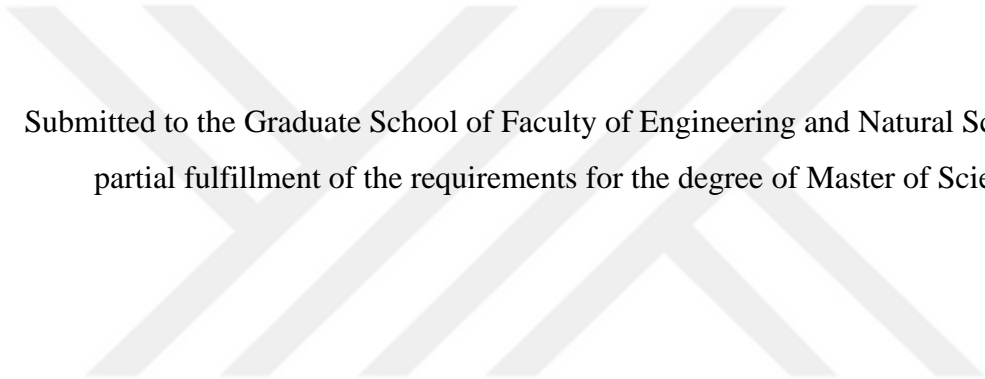
Submitted to the Graduate School of Faculty of Engineering and Natural Sciences in partial fulfillment of the requirements for the degree of Master of Science

Sabanci University

Fall 2021

December 17, 2021

A NOVEL STAPHYLOCOCCUS AUREUS-MODIFIED ELECTROCHEMICAL
BIOSENSOR FOR DETERMINATION OF HEAVY METALS IONS

APPROVED BY:
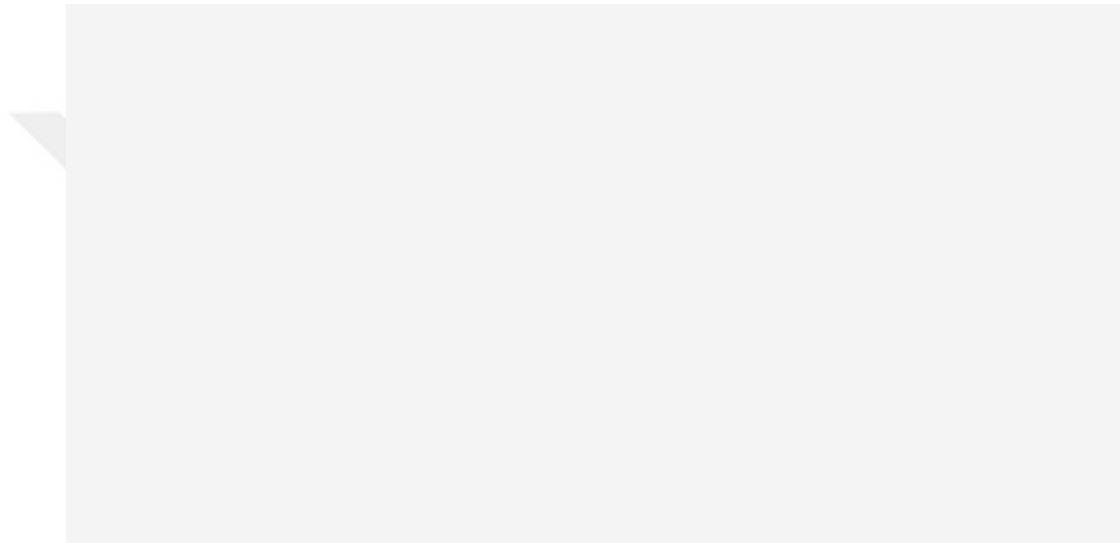
DATE OF APPROVAL: ....
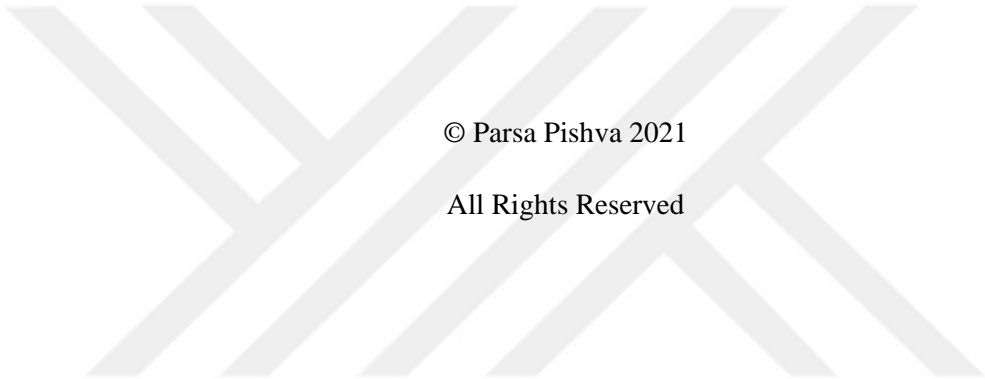
A NOVEL STAPHYLOCOCCUS AUREUS-MODIFIED ELECTROCHEMICAL BIOSENSOR FOR DETERMINATION OF HEAVY METALS

Parsa Pishva

Materials Science and Nanoengineering, MS Thesis, 2021

Dr. Meral Yuce

Cd sensor, heavy metal sensing, electrochemical sensor, microbial detection, Staphylococcus aureus

Heavy metals, even in low concentrations, can harm living organisms. Therefore, in this research, the dried *Staphylococcus aureus*-modified carbon paste electrode's ability to detect different heavy metals ions in three different buffers, including Tris-HCl, sodium acetate, and phosphate-buffered saline (PBS), at pH 6 and 7 were investigated. Using cyclic voltammetry (CV), the capability of the modified biosensor for detecting Cd(II) ions was clearly shown. The effects of buffer pH and preconcentration time on the performance of the developed biosensor for detecting Cd(II) were also studied. CV results showed that the PBS at pH 6 resulted in the peak with the highest peak current (3 µA). Therefore, this buffer was selected as the primary buffer for carrying out the rest of the experiments to detect Cd(II). Among four different preconcentration times, 15 minutes was the optimum one according to both CV and differential pulse anodic stripping voltammetry (DPASV) results. Scanning electron microscopy (SEM), energy-dispersive X-ray spectroscopy (EDX), and Fourier-transform infrared (FTIR) spectroscopy results of modified carbon paste also confirmed the adsorption of Cd(II) ions. According to the FTIR spectrum, phosphate groups played an important role in accumulating Cd(II) ions. The control experiment performed using unmodified carbon paste showed no response to Cd(II) ions. Finally, using the calibration curve, the biosensor's limit of detection and sensitivity were calculated as 45 nM (5.4 µg/L) and 7.61814 µA/µM, respectively, and its linearity was within the range of 100 nM (0.011 mg/L) to 2 µM (0.22 mg/L).

TABLE OF CONTENTS

LIST OF TABLES

LIST OF FIGURES

LIST OF ABBREVIATIONS

PBS: Phosphate-buffered saline

S. aureus: Staphylococcus aureus

CV: Cyclic voltammetry

DPASV: Differential pulse anodic stripping voltammetry

SEM: Scanning electron microscopy

EDX: Energy-dispersive X-ray spectroscopy

FTIR: Fourier-transform infrared

LoD: Limit of detection

LTAs: Lipo-teichoic acids

WTAs: Wall teichoic acids

Cd: Cadmium

Co: Cobalt

Cu: Copper

Ni: Nickel

Pb: Lead

Zn: Zinc

1 INTRODUCTION

1.1 Heavy Metals

All toxic metals are called heavy metals without considering their atomic mass or density. Heavy metals can be transition metals, metalloids, lanthanides, and actinides [1]. However, due to their atomic density greater than 4 g/cm^3, transition metals such as copper, cadmium, lead, and zinc are mainly considered heavy metals causing environmental pollution [1,2]. It is worth mentioning that all living organisms need some specific concentrations of heavy metals, such as cobalt, manganese, iron, copper, zinc, and molybdenum, which humans also require [1,3]. However, High concentrations of these heavy metals can damage different living organisms [4]. Some other heavy metals, including mercury, plutonium, and lead, are toxic at any amount, and their accumulation can cause severe illnesses in living organisms [1]. Accumulation of heavy metals can severely damage the function of different organs such as the heart, brain, kidney, and liver. Moreover, heavy metals can remove essential nutritional minerals from their place in living organisms, disrupting different organs functions [1]. Heavy metals can enter the human body by ingestion, inhalation, and skin contact and cause nausea, vomiting, allergic reactions, reduced growth, and cancers [5]. For instance, Cd(II) is a carcinogen element preventing repairing the errors resulting in DNA mismatches by inhibiting the enzymes [6]. Moreover, the Cu(II) and Fe present in the cytoplasmic can be replaced by Cd(II) due to their inability to produce free radicals. Therefore, the increase in Fe and Cu(II) concentration results in oxidative stress by hydrogen peroxide production [7].

1.2 Heavy Metals Determination

Determination of heavy metals, such as Cd, Cr, Pb, Cu, and Fe, in environment control is of vital importance due to their hazardous properties causing environmental pollution and illnesses for different living organisms [8,9]. According to the World Health Organization (WHO) chemical fact sheets, there are specific limits for heavy metals concentrations in drinking water. For example, the guideline value of Cd(II) presence in drinking water is 0.003 mg/L [10].

Spectroscopic techniques, X-ray fluorescence, and neutron activation analysis are the most versatile methods for detecting heavy metals because of their advantages, such as good sensitivity and femtomolar range LoD [5,11,12]. However, these methods need

control of laboratory setting and complex instrumentation, resulting in high costs and *in situ* application problems. Therefore, researchers have been looking for new methods to overcome these drawbacks [13,14].

On the other hand, electrochemical methods and devices have numerous advantages, such as being simple, user-friendly, cheap, and suitable for *in situ* measurements, making them an effective alternative for mentioned methods [5]. Moreover, since electrochemical methods require minimal sample changes, contamination and losses due to adsorption by containers are significantly reduced. Fast testing and real-time data gathering are also other advantages of electrochemical devices and methods [5]. However, more effort has to be still put into improving these devices to optimize their sensitivity and LoD [5].

Cyclic voltammetry (CV), square wave voltammetry (SWV), linear sweep voltammetry (LSV), and differential pulse voltammetry (DPV) are different voltammetry methods that can be employed for detecting heavy metals [15]. The main difference between these voltammetry techniques is the time waveforms produced by the respective functional application, and SWV and DPV are the most sensitive voltammetry methods [15,16]. A standard electrochemistry system has a potentiostat, detection instrument, and electrolyte. The electrochemical detection system consists of three electrodes which are working electrode (WE), reference electrode (RE), and counter electrode (CE). Working electrodes can be employed for detecting different heavy metal ions [15,17].

Even though it has been reported that mercury electrodes can be successfully employed for the detection of heavy metals [18], their toxicity has limited their application [19]. Therefore, they have been replaced by other electrodes such as carbon, gold, platinum, iridium, and silver electrodes [20].

Employing carbon electrodes for electrochemical detection of heavy metals is one of the best alternatives for previous methods due to the carbon's fast electron transfer rate, high electrical conductivity, and chemical stability [21]. Therefore, Researchers have employed different allotropes of carbon to fabricate electrodes to detect heavy metals by electrochemical techniques [22]. Since graphite and glassy carbon are great conductors, they are the best options for fabricating electrodes and detecting heavy metals [22]. Screen-printed carbon electrodes (SPCE), glassy carbon electrodes (GCE), and carbon paste electrodes (CPE) are the most common carbon-based electrodes that can be used for this purpose [22].

2

Zhao *et al.* investigated the detection of Cu(II), Pb(II), Cd(II), and Zn(II) at different concentrations in acetate buffer by electrochemical methods using carbon nanotubes [21]. Figure 1 [21] shows the anodic stripping peaks and calibration curves of Cu(II), Pb(II), Cd(II), and Zn(II) at different concentrations. The anodic stripping peaks were obtained at 24mV, -488mV, -716mV, and -980mV, respectively. Cu(II) and Pb(II) peaks were sharper than Cd(II) and Zn(II) peaks. It was reported that Cu(II), Pb(II), Cd(II), and Zn(II) peaks could be obtained at potentials more negative than -0.3 V, -0.7 V, -0.9 V, and -1.2 V, respectively. However, more negative deposition potentials decreased peak currents because of the hydrogen evolution, which decreased the active electrode surface (Figure 2a) [21]. Moreover, it was shown that the increase in the deposition time increased the sensitivity of the carbon nanotubes for detecting Cu(II), Pb(II), Cd(II), and Zn(II), which was related to the increase of the amount of ion deposition on the electrode surface (Figure 2b) [21].
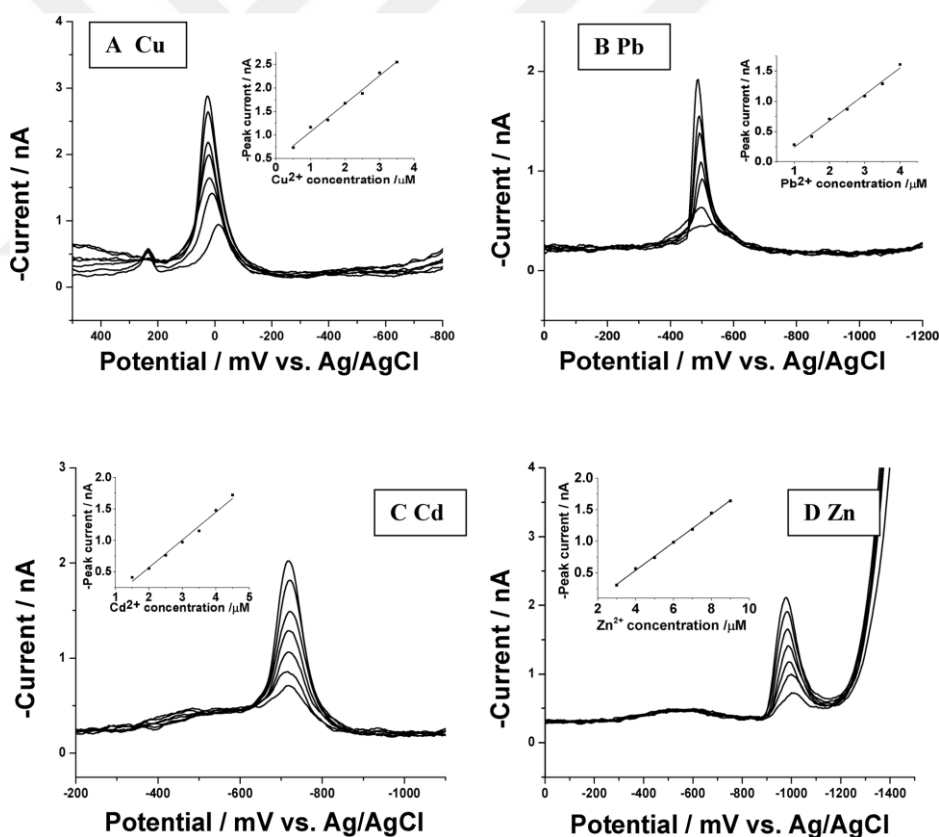
Figure 1. Anodic stripping voltammetry and calibration curves of Cu(II), Pb(II), Cd(II), and Zn(II) in acetate buffer [21].
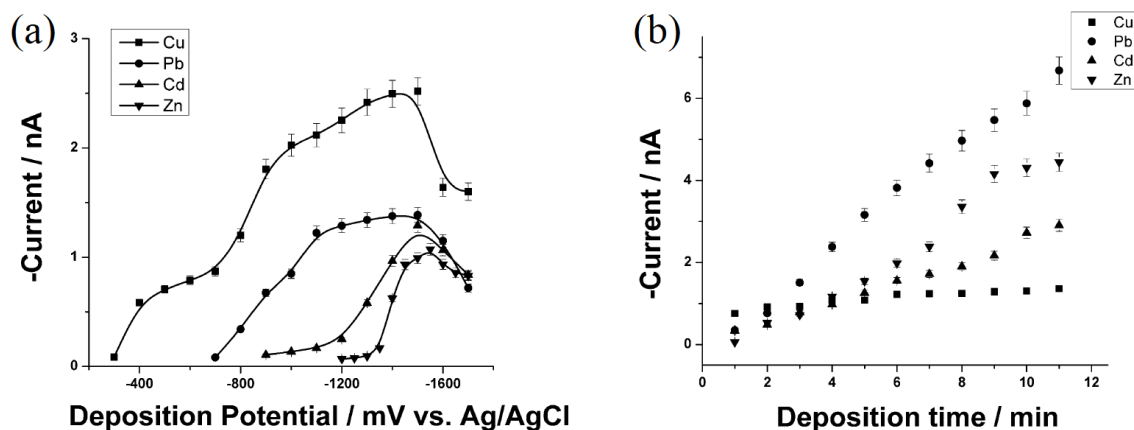
Figure 2. Effect of (a) deposition potential and (b) deposition time on the peak current of Cu(II), Pb(II), Cd(II), and Zn(II) in acetate buffer [21].

Promphet *et al.* also fabricated a graphene/polyaniline/polystyrene nanoporous fibers modified electrochemical sensor using electrospinning for the detection of Pb(II) and Cd(II) at the same time [23]. First of all, the optimum amount of graphene was investigated. For this purpose, a standard solution of 1 mM $[Fe(CN)_6]^{4-/3-}$ in 0.5 M KCl and CV technique were used. According to Figure 3 [23], the increase in the graphene amount from 0 to 4 mg/mL increased the anodic peak current. However, for graphene amounts greater than 4 mg/mL, a reduction in the anodic peak current was observed again that was related to the self-agglomeration of graphene in the fibers, resulting in decreased surface area and electrical conductivity [23].
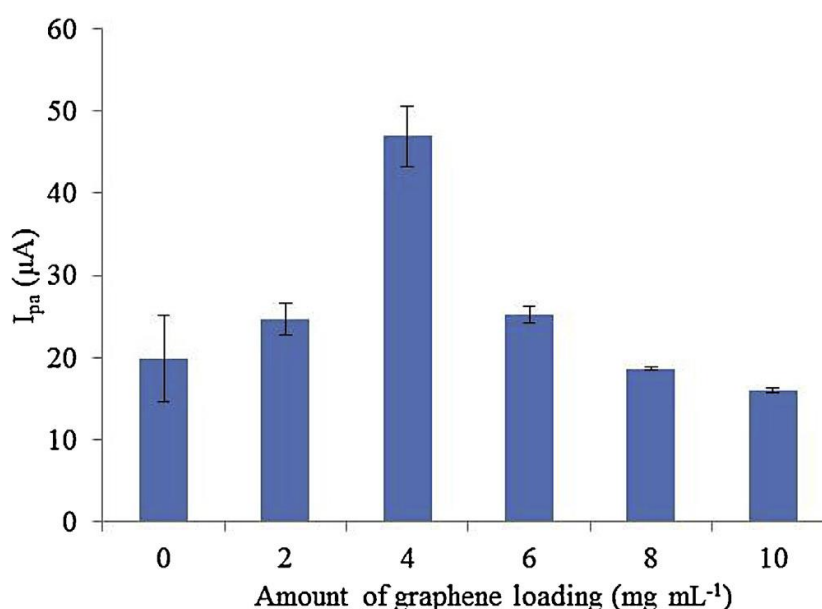
Figure 3. Effect of the amount of graphene on CV peak current obtained from the standard solution of 1 mM $[Fe(CN)_6]^{4-/3-}$ in 0.5 M KCl [23].

4

Other parameters, including the buffer solution, deposition potential and time, potential amplitude, and step potential, were also optimized to obtain the highest anodic peak current for simultaneous detection of Cd(II) and Pb(II). HCl was selected as the buffer solution, and frequency, potential amplitude, and step potential were 100 Hz, 40 mV, and 21 mV, respectively [23]. Different deposition potentials and times were also tested to determine optimum deposition potential and time. According to Figure 4a, the increase in the deposition potential from -1 to -1.2 V increased the anodic peak current for both Cd(II) and Pb(II) [23]. However, more negative potentials resulted in less peak current due to the hydrogen evolution that was in agreement with Zhao *et al*. [21] result.

Moreover, the time range from 60 to 300 seconds was chosen to study the effect of deposition time (Figure 4b) [23]. It was shown that the anodic peak current of both Cd(II) and Pb(II) increased with the increase in deposition time from 60 to 180 seconds. However, the peak current decreased slightly when the deposition time increased from 180 to 300 seconds because of the saturation of electrode surface due to absorbing excessive heavy metal ions [23].
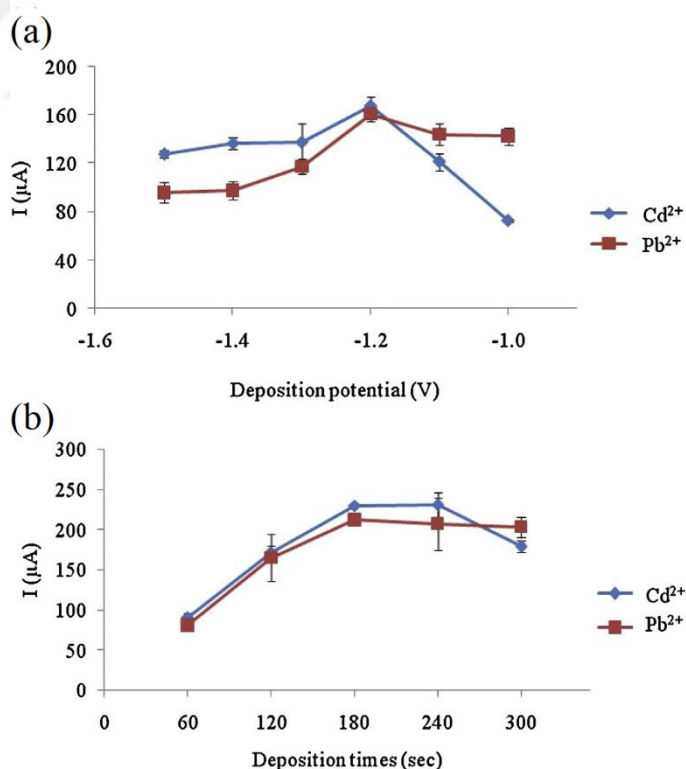
Figure 4. Effect of deposition (a) potential and (b) time on anodic peak current of Cd(II) and Pb(II) detected by a graphene/polyaniline/polystyrene nanoporous fibers modified electrochemical sensor [23].

1.3 Microorganism Modified Electrochemical Biosensors For The Detection of Heavy Metals

1.3.1. Microorganisms

Bacteria, viruses, and fungi are the three main types of microbes [24,25]. Bacteria are microscopically very small, and their diameter or length is generally between 1-2 μm. Viruses are much smaller than bacteria, and their regular size is between 0.2 to 0.02 μm [24,25]. Bacteria do not have a visible internal structure and the nucleus, which is a vital part of the algae, protozoa, and fungi. For this reason, bacteria are called prokaryotes to be distinguishable from nucleate organisms that are called eukaryotes. On the other hand, viruses do not have any cell structure and are simply bundles of genetic information. The genetic information of the bacteria is in a single loop structure [24,25]. Many different species of bacteria usually look the same. However, they usually have three main shapes, including rods (bacilli), spheres(cocci), and commas (vibrios). The cell wall of bacteria, which is a single rigid, mesh-like web, determines the shape of different bacteria [24,25].

One of the most important classifications of bacteria is based on the Gram stain, which classifies the bacteria according to their cell envelope [26]. The cell wall thickness of the gram-positive bacteria is within the range of 20-80 nm, while the cell wall of gram-negative bacteria is thinner, and its thickness is less than 10 nm [26]. However, gram-negative bacteria have an outer membrane that has several pores and appendices (Figure 5) [26]. In other words, gram-positive bacteria have a thicker peptidoglycan wall. However, the peptidoglycan layer of the gram-negative cell wall is covered with an outer lipid bilayer membrane [26].

S. aureus is one of the 32 species of the Staphylococcus genus bacteria. Even though the origin of this bacteria is not clear, some researchers believe that it has evolved from prehistoric soil bacteria. This bacterium cannot move and grows in clusters like grapes whose shapes are perfectly spherical (Figure 6) [27]. Its cells are 1 μm in diameter [27].
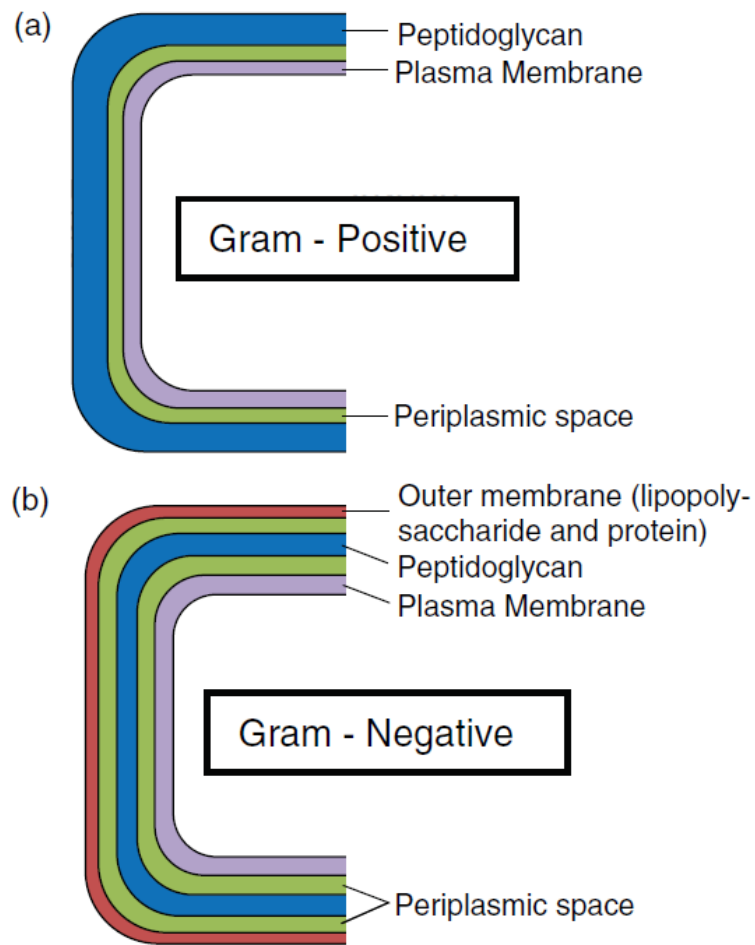
Figure 5. Schematic demonstration of (a) gram-positive and (b) gram-negative bacteria [28].

Figure 6. An SEM image of *S. aureus* showing bacteria's spherical shape growing in grape-like clusters [27].

1.3.2. Biosorption capability of microorganisms

Because of the biosorption capabilities of the microorganisms and their easy and rapid cultivation, they can be successfully used along with carbon for the rapid detection of heavy metals [29]. The biosorption capability of the microorganisms is due to their cell wall components that act as active metal sorption sites [29]. Therefore, employing microbial-modified carbon paste to detect heavy metals at low concentrations has attracted the attention of researchers because of their low cost, high sensitivity, accuracy, and the possibility of in situ analysis [8,13].

Fungal and bacterial biomasses along with carbon paste have been successfully employed to detect heavy metals using electrochemical techniques [8,13,30–32]. It has been well shown that different bacteria and fungi have biosorption capability, allowing them to absorb heavy metals by an active or passive process in the aqueous solutions [13,30–35]. In an active process, the cellular metabolism of bacteria plays a vital role in absorbing ions. In contrast, the cell walls absorb the metal ions in the passive process, and the cellular metabolism has nothing to do with ion absorption [36]. It has been reported that employing heat-dried biomasses makes the electrochemical detection of heavy metals more efficient and straightforward since they possess secondary or latent binding sites that can increment the absorption capability [31]. In other words, dried bacteria absorb heavy metals by a passive process where metal ions bind to cell walls.

In three different studies, Yuce *et al.* investigated the capability of *Rhodotorula mucilaginosa* modified microbial biosensor, an algal sensor, and *Pseudomonas aeruginosa* biomass for detecting Cu(II) and Pb(II) [8,13,31]. The electrochemical tests showed that microbial modified biosensors successfully detected Cu(II) and Pb(II). It was shown that different parameters including scan rate, electrolyte pH, and preconcentration time could affect the sharpness of CV and DPSV peaks [8,13]. For instance, according to Figure 7 [8], the sharpest CV peaks, obtained from *Rhodotorula mucilaginosa* modified biosensor for detecting Cu(II), belong to the scan rate of 100mV/s and 15 minutes of preconcentration [8].

Moreover, It has been reported that pH value can also significantly affect the peak sharpness. According to Figure 8, the optimum pH value for detecting Pb(II) is 8. It was shown by Yuce *et al.* that at very low (acidic) pH values, most of the binding sites on the biosensor's surface could be protonated, decreasing the binding of heavy metal cations to

the surface of the microbial modified biosensor. On the other hand, it was reported that at pH values above 8, peak current started to decrease again due to the reaction between Pb(II) ions and hydroxide, resulting in the insoluble Pb(II) hydroxylic complexes, which prevented binding of Pb(II) on the biosensor's surface. [13].
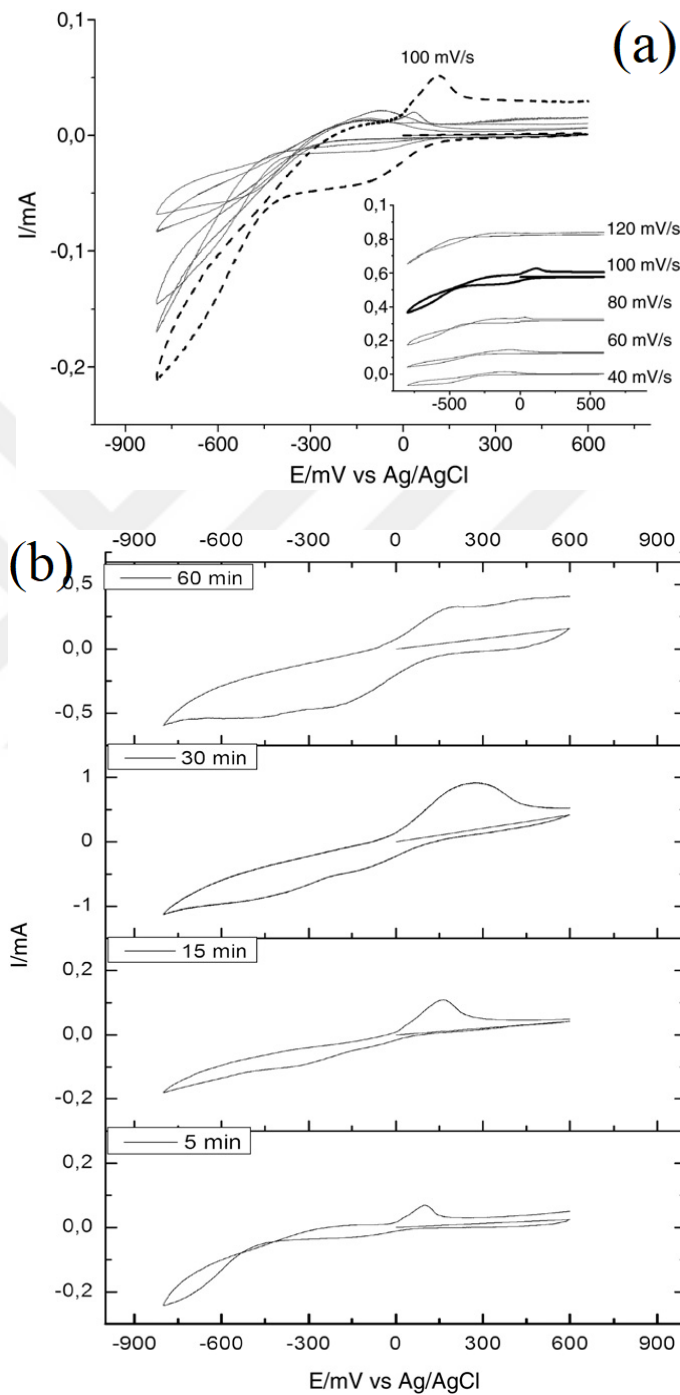
Figure 7. Effect of (a) scan rate and (b) preconcentration time on CV peaks obtained from *Rhodotorula mucilaginosa* modified biosensor for detecting Cu(II) [8].

9
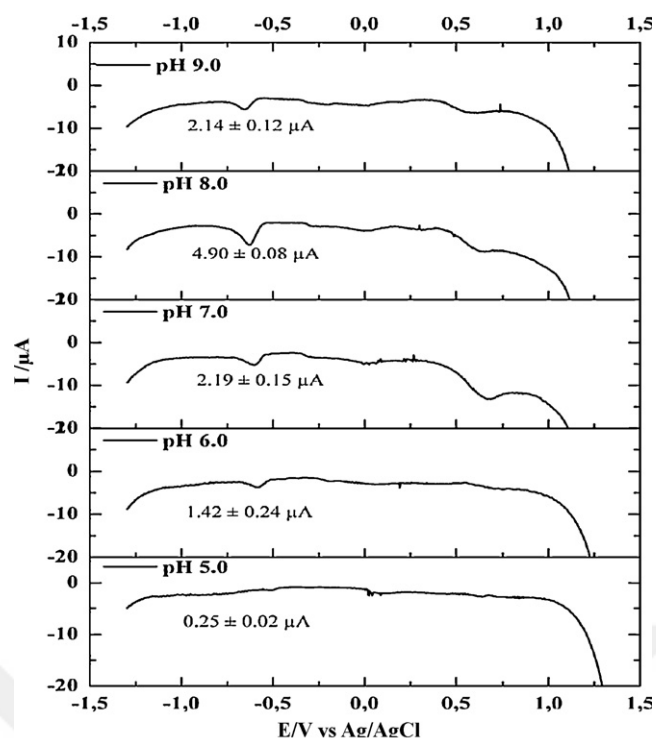
Figure 8. Effect of acetate buffer pH on DPSV peaks of Pb(II) ions determined by *Phormidium sp.* modified electrochemical biosensor [13].

Even though a few mercury and carbon-based electrodes have been used to detect Cd(II) [14,23,37], as far as we know, there is no extensive study on the application of bio-modified carbon paste electrodes for the detection of Cd(II) using electrochemical techniques. Therefore, in this research, the capability of *S. aureus*-modified carbon paste to detect Cd(II) in aqueous media by employing electrochemical methods, including cycling voltammetry (CV) and differential pulse anodic stripping voltammetry (DPASV), has been investigated. As mentioned, because of the graphite's fast electron transfer rate, high electrical conductivity, chemical stability, and lower costs compared to other techniques, this method is investigated as an alternative option for other methods. The reason for choosing *S. aureus* as the modifying microorganism is because it has been shown that dead gram-positive bacteria can passively absorb heavy metal ions [18,38]; however, the capability of electrochemical *S. aureus*-modified carbon paste biosensor for detecting Cd(II) ions has not been revealed before.

2 MATERIALS AND EXPERIMENTS

2.1 Chemicals

The stock solution of Co(II), Cu(II), Cd(II), Zn(II), Pb(II), and Ni(II) (1 M) was prepared using Co(II), Cu(II), Cd(II), Zn(II), Pb(II), and Ni(II) nitrate powder (Sigma Aldrich) and distilled water. By diluting the stock solution using deionized (DI) water, the standard solutions were prepared. Finally, 0.05M Tris-HCl, 0.05M phosphate-buffered saline (PBS), and 0.05M sodium acetate buffers were used to prepare the final electrolyte solution containing 250 nM Cu(II), Co(II), Cd(II), Pb(II), Zn(II), and Ni(II) ions. Tris-HCl buffer was prepared using trizma base (Sigma Aldrich) and hydrochloric acid, PBS buffer was prepared using monobasic potassium phosphate (Sigma Aldrich) and sodium hydroxide (Sigma Aldrich), and sodium acetate buffer was prepared using acetic acid and sodium acetate (Sigma Aldrich). Griphite powder and mineral oil (Sigma Aldrich) were employed to prepare the carbon paste. The *S. aureus* bacteria were cultivated in the broth medium.

2.2 Microorganism Cultivation

In this study, dried *S. aureus* bacteria were used for the modification of the carbon paste electrode. The broth medium was employed to cultivate the microorganism (Figure 9a). For this purpose, the microorganism was incubated for 30 hours at 37°C and 250 rpm using a rotary shaker (Figure 9b). After incubation, the microorganisms were separated from the medium by centrifugation at 5000 rpm for 10 minutes (Figure 9c and d). To wash the obtained microorganisms, they were centrifuged once more using PBS buffer. Finally, the microorganism was dried in an oven at 80°C for 15 hours (Figure 9e and f).

2.3 Preparation of Biosensor

To prepare uniform *S. aureus*-modified carbon paste, dried *S. aureus* bacteria (0.3g), graphite (0.9g), and mineral oil (0.9g) were thoroughly mixed. The ratio of the graphite to the dried-*S. aureus* was 3:1 (0.9g/0.3g). The electrode body was made of Teflon (D=8mm) with a hole (D=4mm) and a Copper rod inside it. The prepared paste was put into the electrode hole with a volume and surface area of 25 mm^3 and 12.5 mm^2 (Figure 10). The surface of the electrode was rubbed against a smooth piece of paper to make the surface smoother after filling the electrode hole with modified carbon paste.
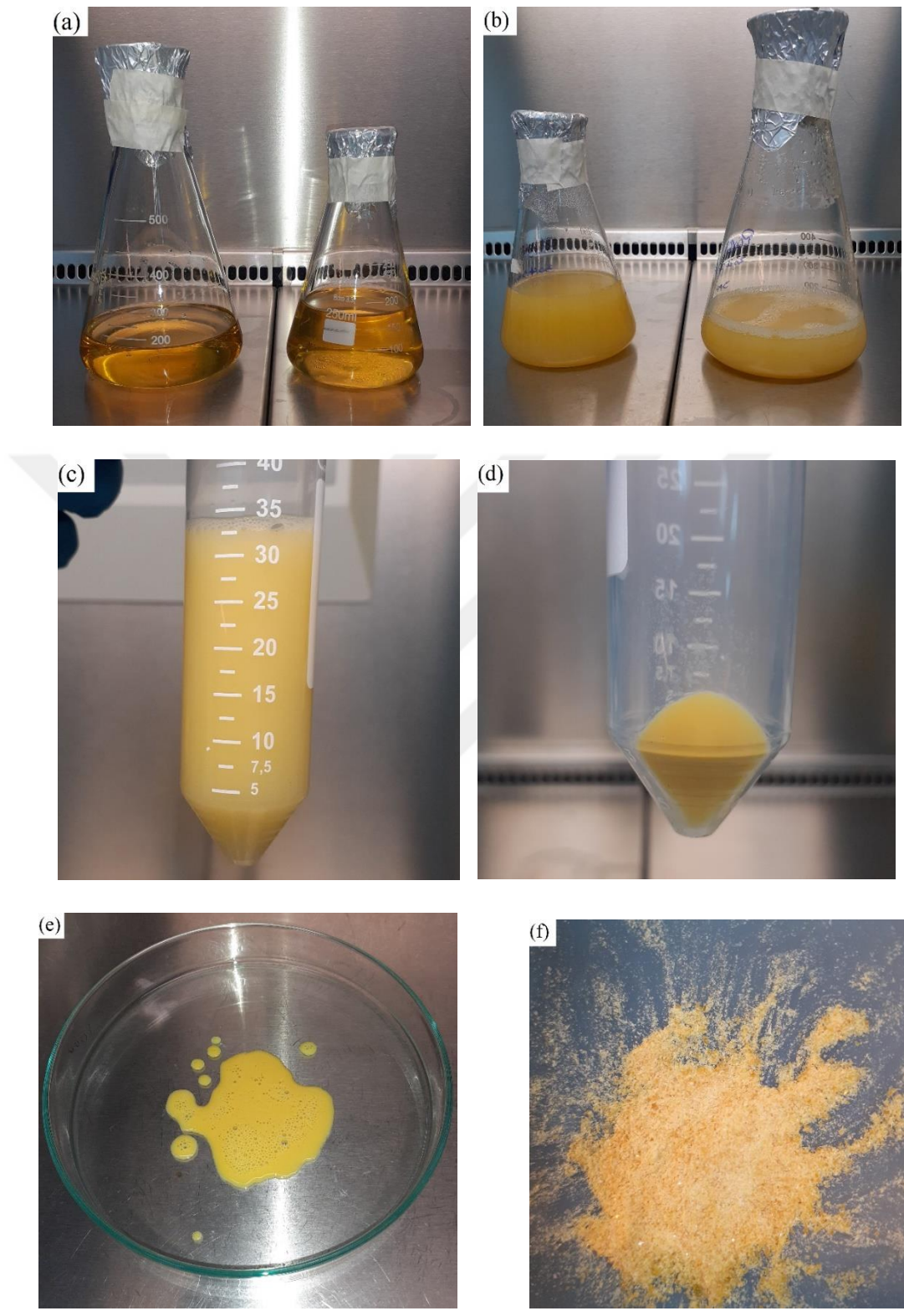
Figure 9. The procedure of microorganism cultivation. (a) The broth medium was used for the cultivation of the microorganism. (b) The microorganism was incubated for 30 hours at 37°C and 250 rpm using a rotary shaker. (c) After incubation, cultivated microorganisms and the broth medium were poured into centrifuge tubes. (d) The microorganisms were separated from the medium by centrifugation at 5000 rpm for 10 minutes. (e) The separated microorganisms

were poured into a glass Petri dish and dried at 80°C for 15 hours. (f) The dried microorganisms were separated from the Petri dish and turned into powder.
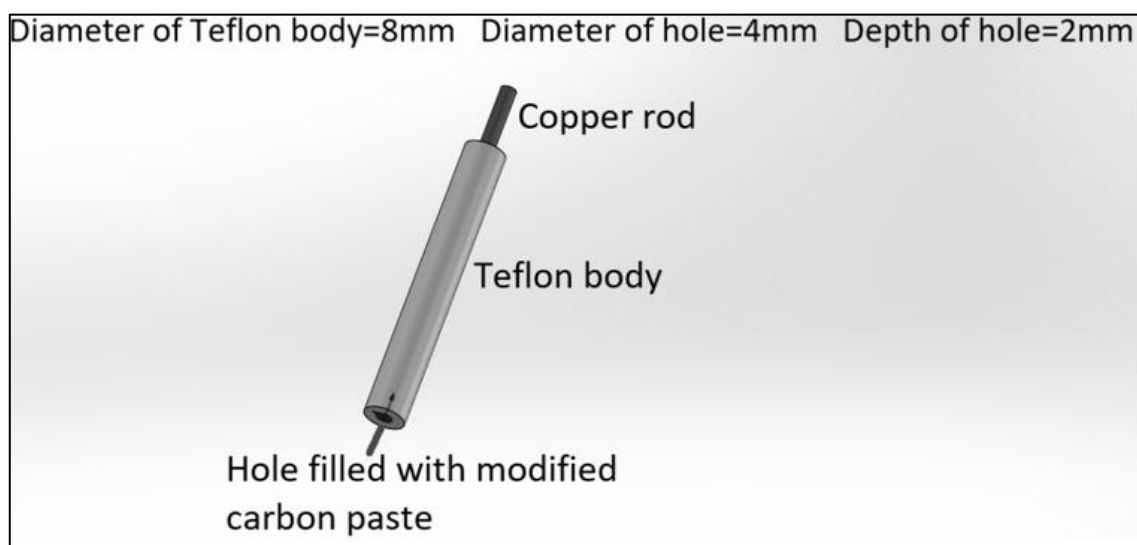
Figure 10. Details of the in-house carbon paste electrode.

2.4 Electrochemical Experiments

A potentiostat device (PARSTAT MC Multichannel Potentiostat) was used for conducting all electrochemical tests using the three-electrode cell at room temperature. The working electrode was the electrode filled with the *S. aureus*-modified carbon paste. The reference and counter electrodes were Ag/AgCl (3.5 M KCl) and platinum, respectively. Each experiment had three steps: 1) preconcentration, 2) medium change, and 3) voltammetric measurements. Open circuit potential (OCP) test was employed for the preconcentration step. For this purpose, the working electrode was immersed in the stirred solution containing 250nM Co(II), Cd(II), Ni(II), Cu(II), Zn(II), and Pb(II) ions, whose pH was measured using a pH meter. Next, the working electrode was removed and washed with distilled water to remove all metal ions that may remain on the electrode. All electrodes were transferred into the three-electrode electrochemical cell where 15 ml of pure Tris-HCl, PBS, and sodium acetate buffers were used without heavy metals ions. Finally, CV measurements were conducted within the potential range of -1.5 to 1.5 V. The scan rates of all CV tests were 10 mV/s. DPASV experiments were also carried out within the potential range of -1.5 to 1.5 V and at the scan rate of 10 mV/s. Pulse height, pulse width, step height, and step width were 1 mV, 0.1 s, 5 mV, and 0.5 s, respectively.

2.5 SEM and FTIR Studies

The morphology and elemental analysis of the bare and *S. aureus*-modified carbon paste, which were immersed in the stirred solution containing 250nM Cd(II), ions for 15 minutes, were carried out using SEM and EDX (FE-SEM, LEO Supra VP-35) (Figure 11a).

FTIR spectra (Thermo-Nicolet iS10 FTIR) (Figure 11b) were also carried out to examine different chemical groups and bands of the *S. aureus*-modified carbon paste before and after loading Cd(II).
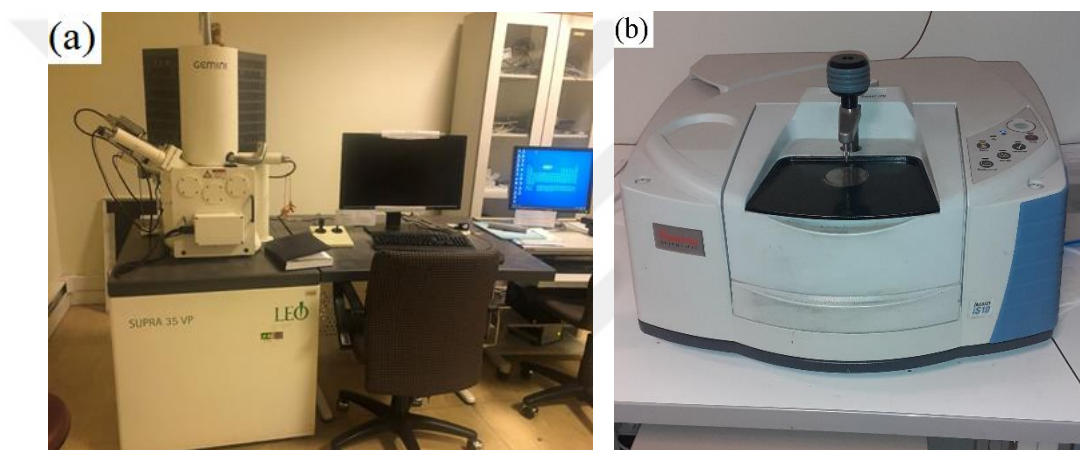
Figure 11. (a) SEM and (b) FTIR devices used to characterize biosensors.

3 RESULT AND DISCUSSION

3.1 Cyclic Voltammetry and Differential Pulse Stripping Voltammetry Experiments

A schematic illustration for the electrode preparation stages was presented in Figure 12. Three different buffer media (sodium acetate, Tris-HCl, and PBS) containing 250 nM Cd(II), Co(II), Cu(II), Ni(II), Pb(II), and Zn(II) ions were tested to compare the CV results using an *S. aureus*-modified microbial biosensor at the scan rate of 10 mV/s and after 15 minutes of preconcentration time (Figure 13a-f). According to the obtained results, all buffers containing 250 nM Co(II), Cu(II), Ni(II), Pb(II), and Zn(II) ions did not have any anodic or cathodic peaks; however, PBS buffer at both pH values (6 and 7) containing Cd(II) ions showed almost sharp anodic peaks. Two anodic peaks with less sharpness can also be seen in CV curves obtained from Tris-HCl and sodium acetate buffers containing Cd(II) ions at pH 6. The formation of metal complexes such as metal acetates and phosphates and the competitive binding of heavy metal ions and other protons and cations present in the buffers with the binding sites on the biosensor surface can be the reasons preventing the detection of Pb(II), Co(II), Ni(II), Zn(II), and Cu(II) [13,39].

As it can be seen in Figure 14a and Figure 14b, the sharpest anodic peak for Cd(II) was obtained in the PBS buffer at pH 6 within the potential range from -0.9 to -0.7 V. Other researchers such as Koudelkova *et al.*, Zheng *et al.*, Baldrianova *et al.*, and Hu *et al.* also reported the same potential range [39–42]. However, the unmodified carbon paste could not detect Cd(II) ions at the same concentration. The *S. aureus*-modified biosensor could detect Cd(II) ions due to the dried *S. aureus'* cell wall components that act as metal sorption sites [29]. Since in this study dried *S. aureus* is employed, there is no active metal absorption process based on the cellular metabolism of bacteria. Here, the passive metal absorption process, where the cell walls absorb the metal ions, and the cellular metabolism has nothing to do with ion absorption, plays a critical role in detecting Cd(II) ions [36]. Therefore, the modified carbon paste electrode can detect a higher amount of Cd(II) ions because the anionic moieties present in the extracellular surface of microorganisms provide binding sites for metallic cations [43].
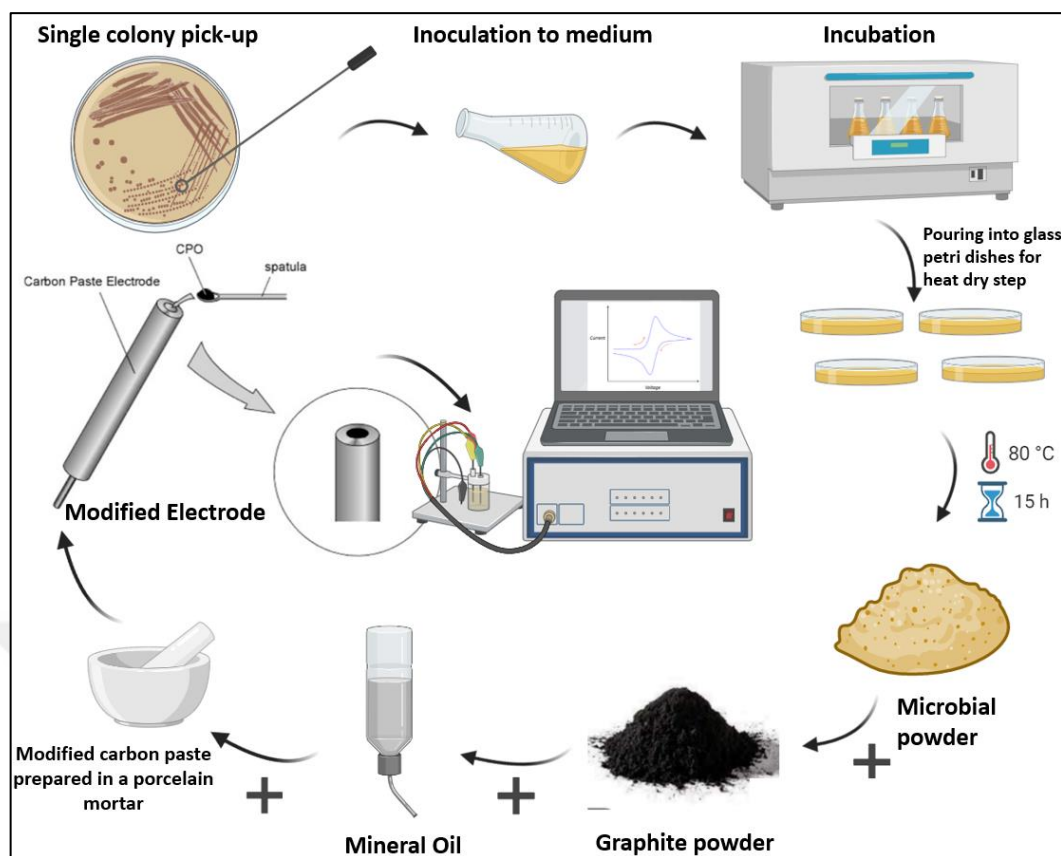
Figure 12. Schematic illustration of the experimental process for sensor surface development

It has been reported that the affinity of the gram-positive bacteria for binding divalent cations is higher than their affinity for binding monovalent ones except for H^+, that is because of the lower mobility of the bound divalent cations compared to monovalent cations [44]. Moreoevr, divalent cations can be absorbed more easily by gram-positive bacteria like *S. aureus* because all vital cations for these bacteria are divalent cations, including Mg^{2+} and Ca^{2+}. Teichoic acid is a flexible biopolymer that is one of the main components of the cell wall of gram-positive bacteria. One of the main functions of teichoic acid is metal cation binding. Teichoic acid has some phosphate groups that help it bind divalent metal cations [45]. Highly charged teichoic acid (anionic polyelectrolytes) forms around 60% of the gram-positive bacteria cell walls. There are two types of teichoic acids containing lipo-teichoic acids (LTAs), connected to the cytoplasmic membrane, spread into the peptidoglycan layer and the wall teichoic acids (WTAs) that are directly attached to the peptidoglycan and continue through the cell wall. Since these teichoic acids are anionic polyelectrolytes in the peptidoglycan, only binding cations, especially divalent ones, can balance the repulsion between them. Moreover, teichoic acids play an essential role in absorbing cations that are vital to the gram-positive bacteria [46].

16

Figure 15 shows the structure of the wall of *S. aureus*. The spatial location of a polyelectrolyte that can be considered independently is defined by a mesh size of length L that is considered constant. Since a single polyelectrolyte contains N monovalent anions (q), its charge line density is Nq/L. Divalent cations bound to the cell wall surround these monovalent anions and are restricted inside a volume V_{poly} in the polyelectrolyte [46]. Figure 15b shows the distribution and condensation of the divalent cations within the *S. aureus* cell wall. Therefore, it can be concluded that the anodic peaks in the CV results appeared due to these bound and restricted Cd(II) cations inside the *S. aureus* cell wall.

According to these figures, even though the *S. aureus*-modified carbon paste could also detect Cd(II) in Tris-HCl and sodium acetate buffers, the peaks are not as sharp as those obtained in the PBS buffer pH 6. The peak sharpness reduction in the sodium acetate buffer can be related to the formation of cadmium acetate complex preventing the detection of Cd(II) [39]. In other words, the formation of Cd(II) complexes with acetate ions decreases the concentration of free Cd(II) ions leading to lower peak intensity [39]. Moreover, the competitive binding of Cd(II) and other protons and cations present in Tris-HCl buffer with the binding sites on the biosensor surface might result in peaks with lower intensity in this buffer [13].
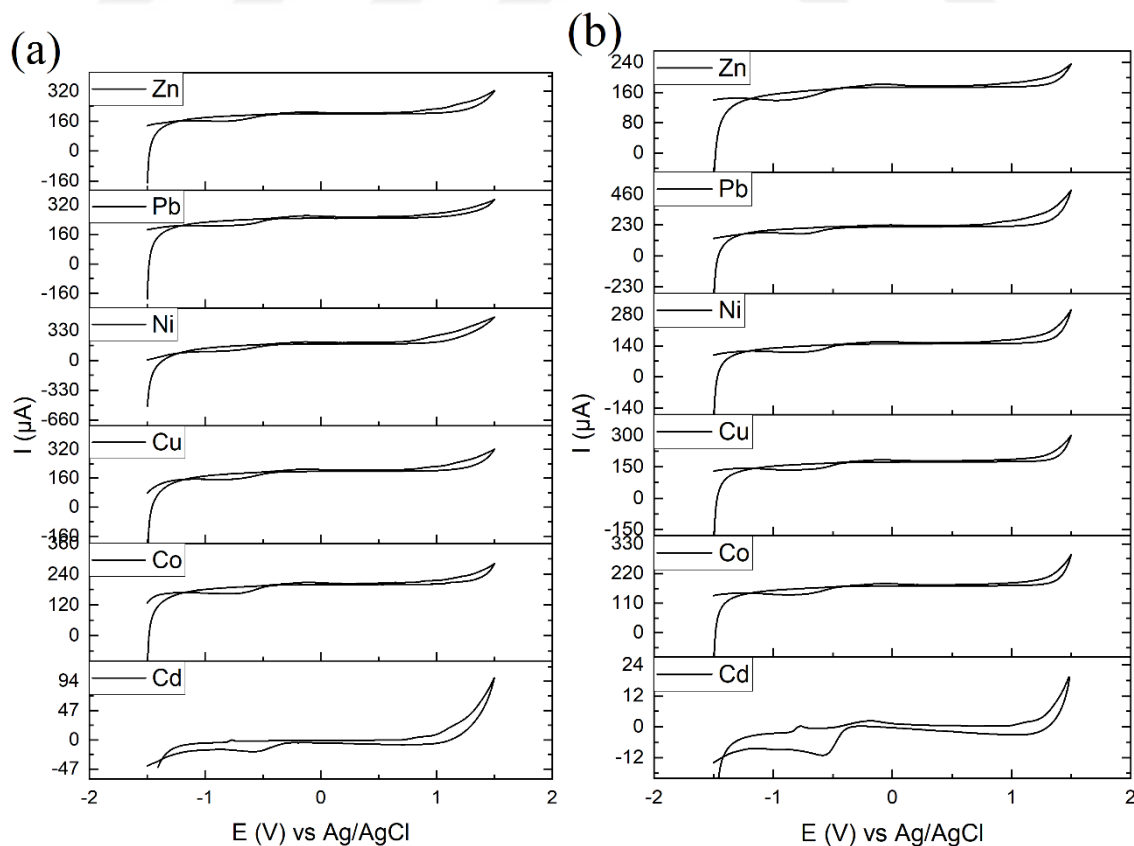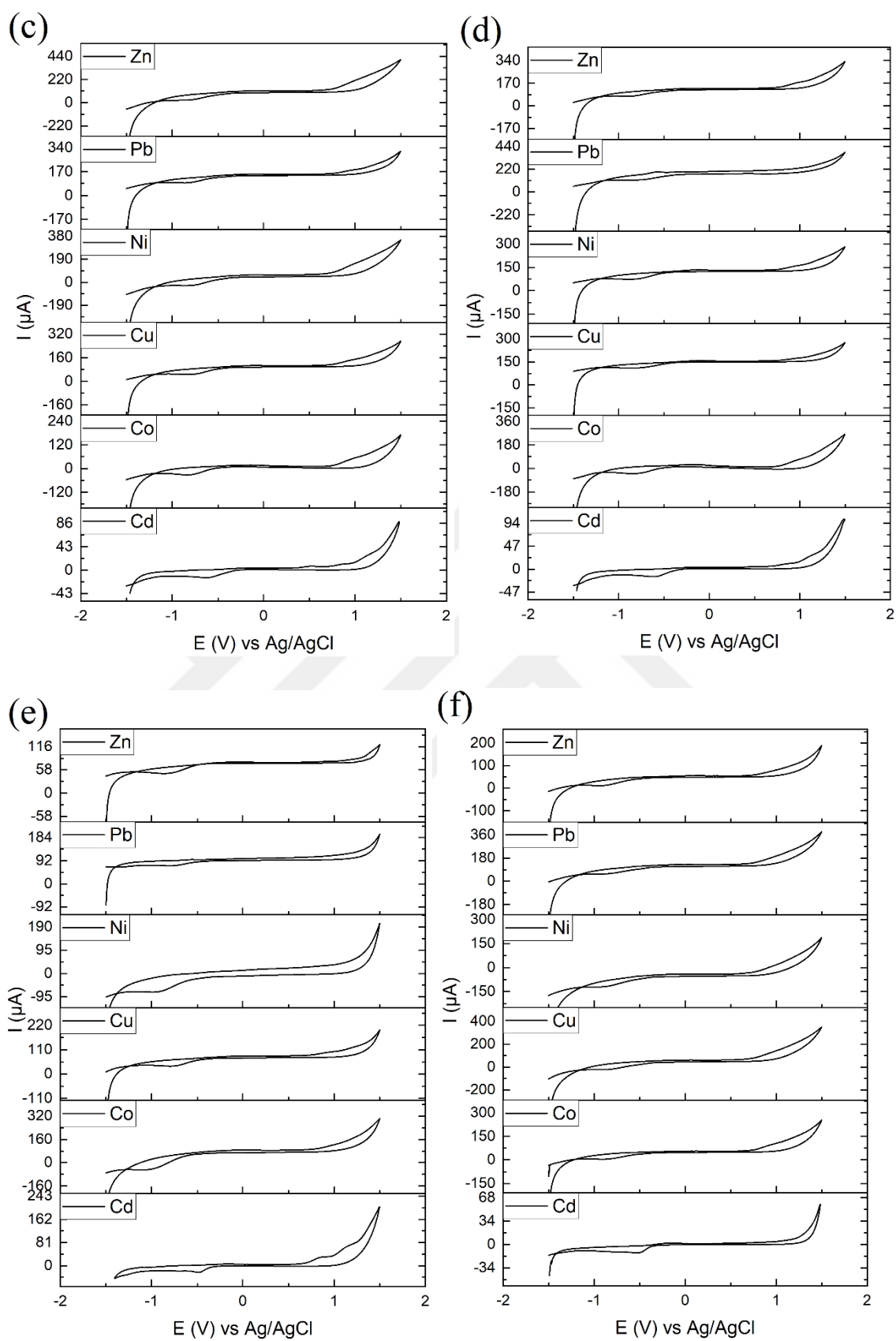
Figure 13. CV curves obtained in (a) PBS pH 6, (b) PBS pH 7, (c) sodium acetate pH 6, (d) sodium acetate pH 7, (e) Tris-HCl pH 6, and (f) Tris-HCl pH 7 containing 250 nM Cd(II),

Co(II), Cu(II), Ni(II), Pb(II), and Zn(II) ions using the *S. aureus*-modified carbon paste after 15 minutes of preconcentration time, at the scan rate of 10 mV/s and the pH levels of 6 and 7.

Another point seen in Figure 14a and Figure 14b is that pH 6 resulted in sharper peaks in all buffers compared to pH 7 because, at pH 7, Cd(II) has a higher tendency to hydrolyze. Consequently, the peak sharpness decreases [43]. It is worth mentioning that lower pH levels can also reduce the peak height since there will be more hydrogen ions competing with Cd(II) ions for being absorbed by binding sites on the modified carbon paste surface. Therefore, at lower pH levels, more binding sites can be occupied by hydrogen ions [13,47].

Following the selection of the most appropriate buffer and optimum pH, four different preconcentration times, including 10, 15, 20, and 25 minutes, were employed to investigate their effects on the detection of Cd(II) ions (Figures 16a and 16b). According to the CV results, the peak sharpness increases as the preconcentration time increases from 10 to 15 minutes. The reason for this increase is the absorption of more Cd(II) ions with increasing time. In other words, since the biosensor is exposed to the electrolyte for a longer time, the chance to absorb more Cd(II) ions increases [8,48]. However, as the preconcentration time increases from 15 to 25 minutes, the peak current decreases indicating that binding sites on the biosensor surface reach their maximum absorption capacity after 15 minutes [8,48].

As shown in Figure 16c and Figure 16d, the same buffer, pH, and preconcentration times were tested using DPASV to confirm the results obtained from the CV test. As it can be seen, the DPASV results are in complete agreement with CV results, confirming that exposing the modified carbon paste to the electrolyte containing 250 nM Cd(II) for 15 minutes in PBS buffer results in the maximum peak current.
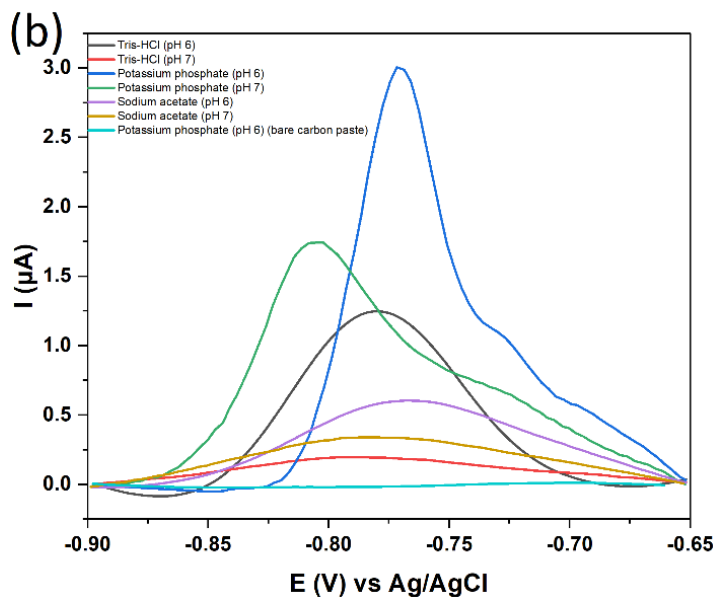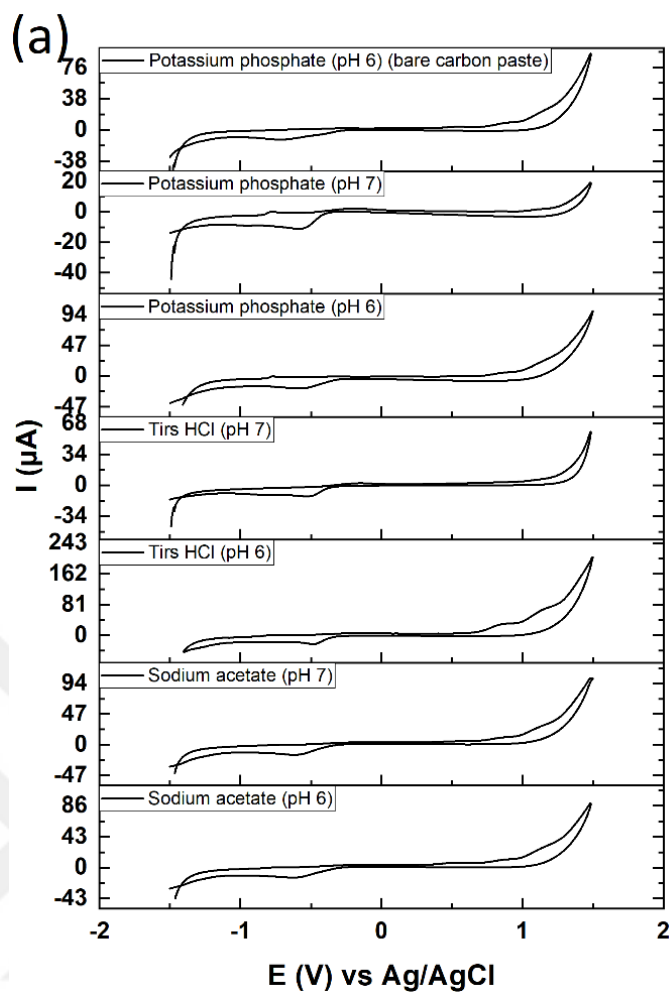
Figure 14. (a) CV curves and (b) enlarged CV anodic peaks obtained in sodium acetate, Tris-HCl, and PBS buffers containing 250 nM Cd(II) ions using the *S. aureus*-modified and unmodified carbon paste after 15 minutes of preconcentration time, at the scan rate of 10 mV/s and the pH levels of 6 and 7.
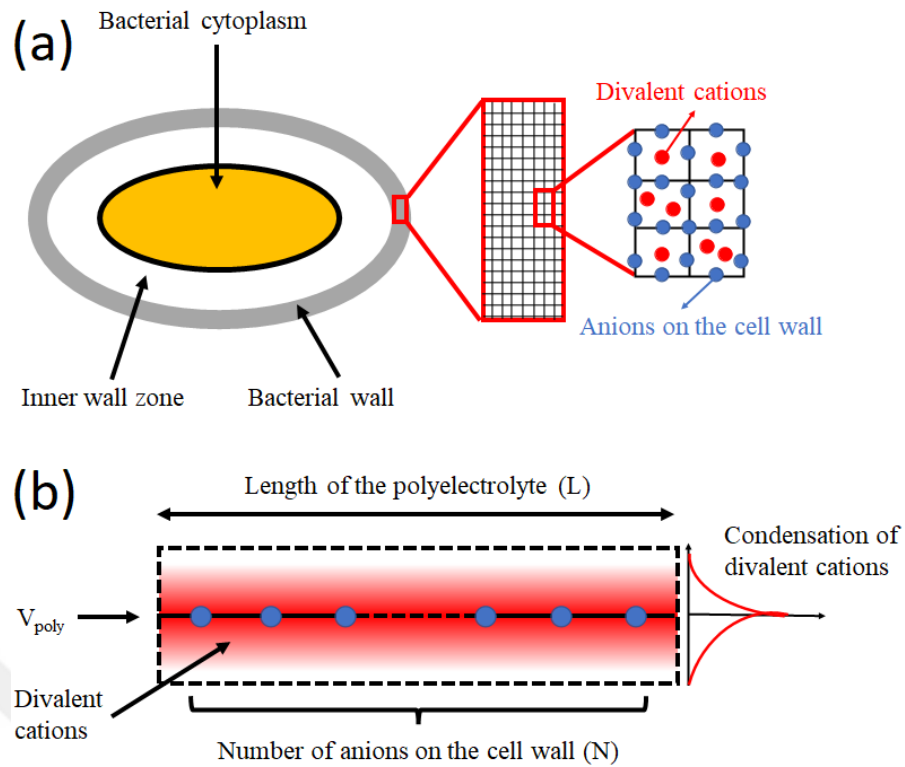
Figure 15. (a) schematic of the *S. aureus* bacteria. The cell wall is considered a polyelectrolyte. Divalent cations surround each monovalent anion on the cell wall. It is assumed that the polyelectrolytes making up one side of the mesh are linear. (b) schematic of the one side of the mesh where cations are condensed within a restricted volume (V_{poly}) close to cell wall anions.
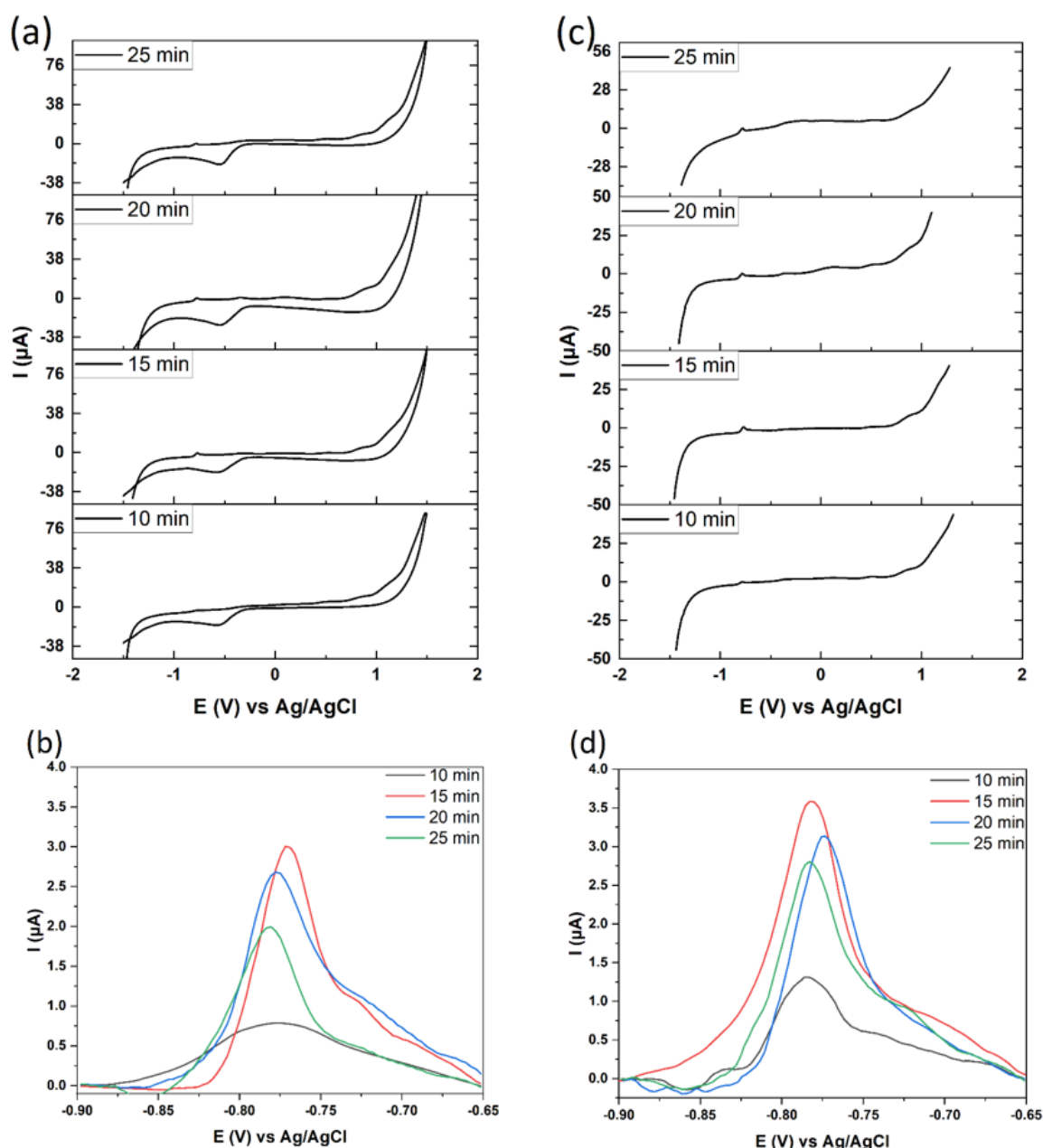
Figure 16. (a) CV curves, (b) enlarged CV anodic peaks, (c) DPASV curves, and (d) enlarged DPASV peaks obtained in PBS buffer containing 250 nM Cd(II) ions using the *S. aureus*-modified carbon paste at the scan rate of 10 mV/s and pH 6.

3.2 SEM and EDX Characterization of the Microbial Cd(II) Biosensor

The SEM micrographs of the *S. aureus*-modified and unmodified carbon paste after loading of 250 nM of Cd(II) and 15 minutes of preconcentration time are shown in Figure 17. As shown by arrows in Figure 16a, bright particles on the surface of the modified carbon paste represent the absorbed Cd(II) ions. However, no absorbed Cd(II) can be seen on the surface of unmodified carbon paste, confirming the electrochemical results. Figure 18a and Figure 18b show the EDX mapping of the *S. aureus*-modified and unmodified

carbon paste, respectively, after loading 250 nM of Cd(II) and 15 minutes of preconcentration time. Moreover, the weight percent of analyzed elements (C, O, and Cd) are provided in Table 1. The results also show the ability of *S. aureus*-modified carbon paste for Cd(II) detection, while the weight percent of Cd in unmodified carbon paste (Figure 18b) was zero.
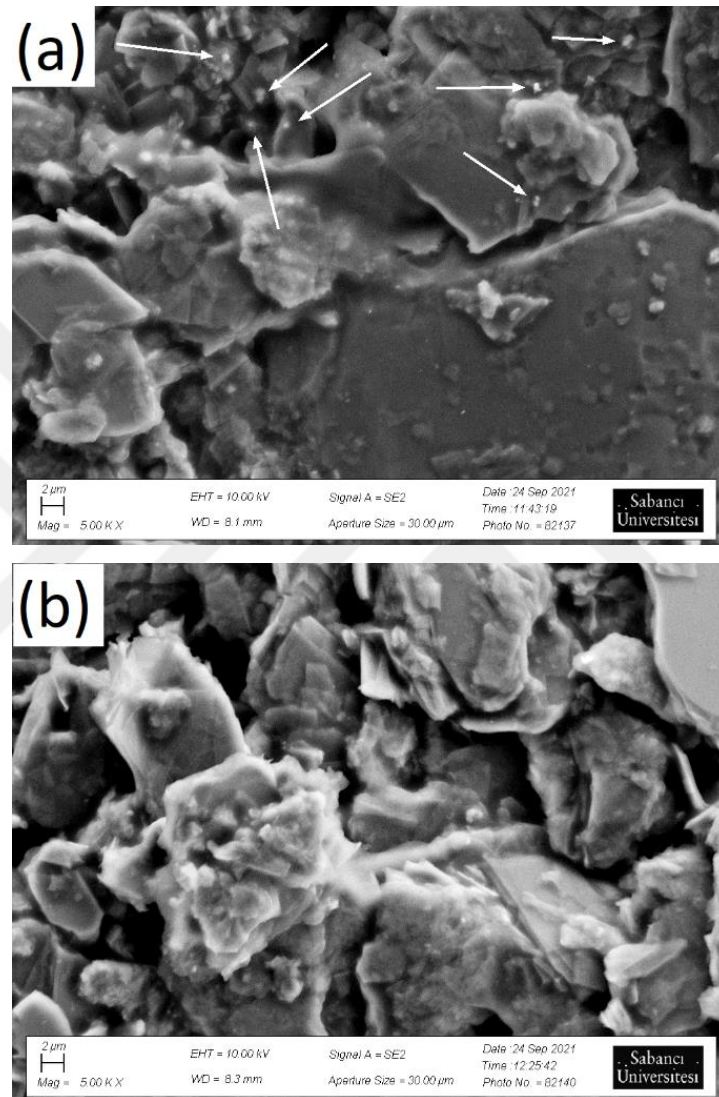
Figure 17. SEM micrographs of the (a) *S. aureus*-modified and (b) unmodified carbon paste after loading of 250 nM of Cd(II). The absorption of Cd(II) ions by *S. aureus*-modified carbon paste is seen in (a).
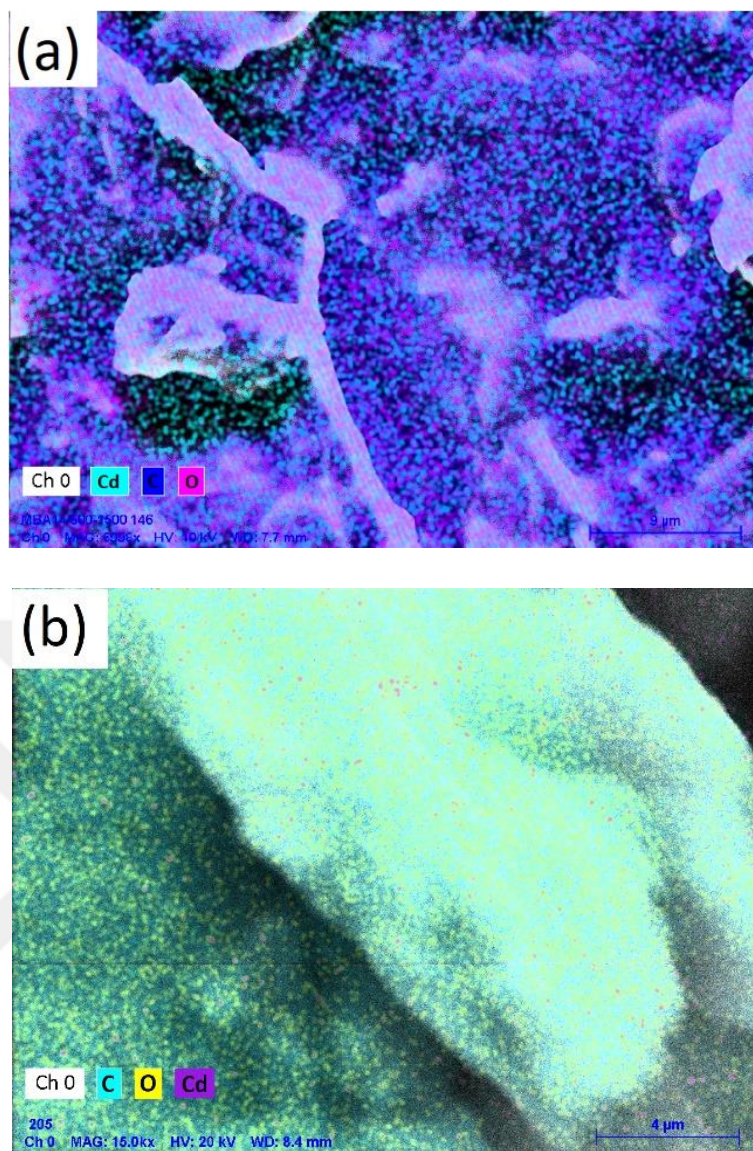
Figure 18. EDX mapping of (a) *S. aureus*-modified and (b) unmodified carbon paste after loading of 250 nM of Cd(II) and 15 minutes of preconcentration time.

Table 1. Elemental analyses of *S. aureus*-modified and unmodified carbon paste after loading 250 nM of Cd(II) ions and 15 minutes of preconcentration time.

S. aureus-modified carbon paste		Unmodified carbon paste	
Element	wt.%	Element	wt.%
C	99.07	C	98.57
Cd	0.15	Cd	0
O	0.78	O	1.43

3.3 FTIR Studies

FTIR spectroscopy of Cd(II) loaded and unloaded (native) *S. aureus*-modified carbon paste is shown in Figure 19 to investigate the interactions between *S. aureus*-modified carbon paste and Cd(II) ions. The broad peak around 3200 cm^{-1} represents bonded O-H and NH$_2$ groups [13,49]. The peaks present around 2850 and 2920 cm^{-1} belong to C-H stretching, and the peak around 1700 and 1505 cm^{-1} represent the C=O and C=C bonds, respectively [49]. There are also two peaks around 1450 and 1400 showing the presence of C-H [9,49]. Moreover, two C-O bond peaks are seen at about 1070 and 1220 cm^{-1} [49]. There is also a narrow peak around 860 cm^{-1} belonging to the PO$_4^{3-}$ [50,51].

One of the most apparent differences between the FTIR spectra of the native and loaded *S. aureus*-modified carbon paste is the reduction in the intensity of the phosphate peak around 860 cm^{-1}, indicating the critical role of this group in the absorption of Cd(II) ions. As mentioned earlier, dried *S. aureus* can absorb Cd(II) ions by the passive metal absorption process, where the cell walls absorb the metal ions. There are three cell wall polysaccharides in *S. aureus*, teichoic acids, teichuronic acids, and other polysaccharides. Ribitol teichoic acid is the major cell wall polysaccharide in *S. aureus* that acts as a phosphate reserve and participates in metal cation absorption due to the presence of the phosphate group [52,53]. It has been well shown that the capacity of the *S. aureus* cell walls for absorbing cations is in the following order: divalent > monovalent [52]. Moreover, it has been reported that most metal cations are absorbed on the outer surfaces of the cell walls since they contain more phosphate and electronegative sites than the inner surfaces [54].

To ensure that a reduction in the intensity of the phosphate peak around 860 cm^{-1} has occurred, it is also essential to compare the ratio of the intensity of this peak to the intensity of other peaks in both FTIR spectra. Since the intensity of the C-H stretching peak around 2920 cm^{-1} has also been reduced dramatically, comparing the ratio of the intensity of this peak to the intensity of phosphate peak before and after the addition of Cd(II) ions can prove the participation of the phosphate group in binding Cd(II) ions on the surface of *S. aureus*-modified biosensor. The ratio of the intensity of the C-H stretching peak to the intensity of phosphate peak before and after the addition of Cd(II) ions is approximately 3 and 10, respectively, confirming the essential role of phosphate groups in detecting Cd(II) ions.
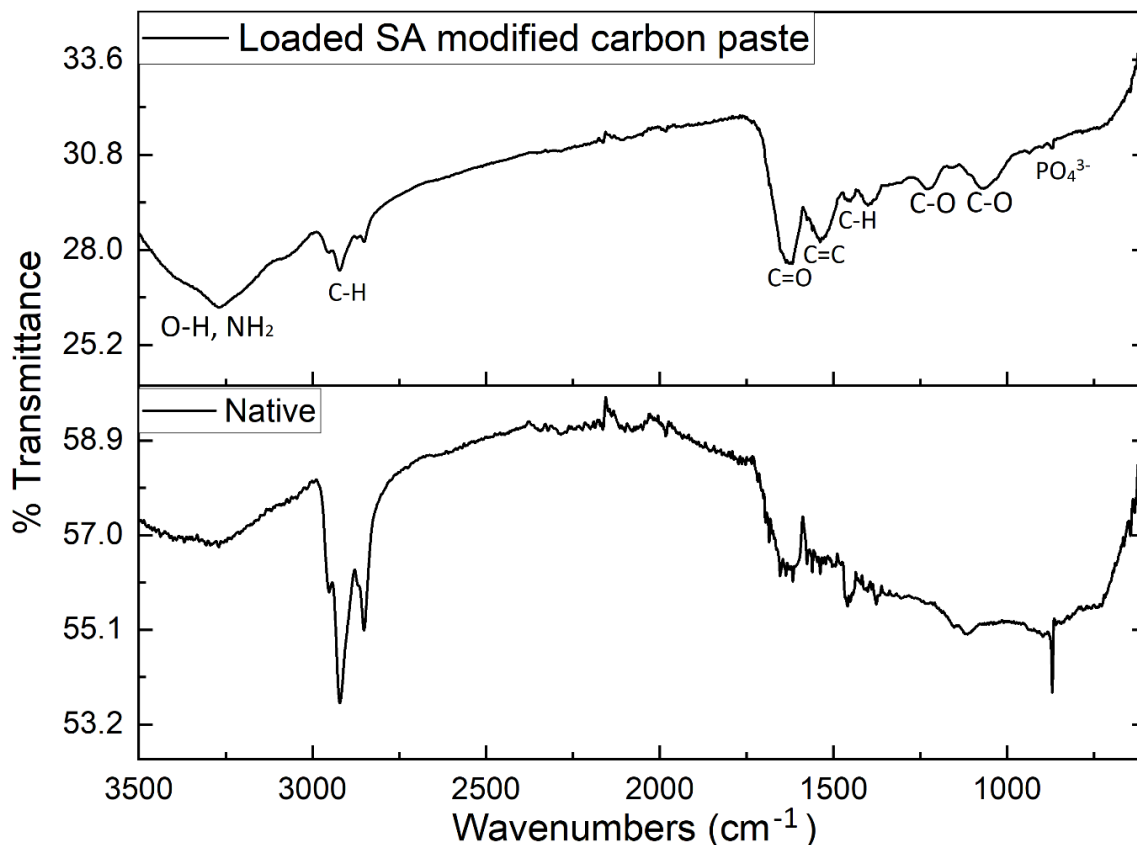
Figure 19. FTIR spectra of the native and Cd(II) loaded *S. aureus*-modified carbon paste.

3.4 Analytical Characteristics of the *S. aureus*-modified Carbon Paste

The optimum conditions (PBS buffer, pH 6, and 15 minutes preconcentration time at open circuit) were employed to conduct DPASV measurements three times for each different concentration (Figure 20a) to plot the calibration curve. As shown in Figure 20b, the increase in the Cd(II) concentration increased the peak current (i_p). However, according to Figure 20c, the linear range of the *S. aureus*-modified biosensor was within the range of 100 nM (0.011 mg/L) to 2 µM (0.22 mg/L). At the concentration of 3 µM, the deviation from the linearity starts, related to the saturation of the binding sites on the surface of the *S. aureus*-modified carbon paste. The line equation and R^2 are y=7.61814x+1.7532 and 0.99, respectively. Moreover, according to the calibration curve, the biosensor's limit of detection and sensitivity for detecting Cd(II) is 48 nM (5.4 µg/L) and 7.61814 µA/µM. Finally, the dynamic range of the developed biosensor is around 2 orders of magnitude (from 48 nM/L to 4 µM/L, or from 5.4 µg/L to 450 µg/L). Recently, Kava *et al.* reported a disposable glassy carbon stencil printed electrode for detecting Cd(II) using electrochemical methods, whose linearity was within the range of 7.5 to 200 µg/L, and

its LoD and sensitivity were 0.46 µg/L and 0.122 µA.L/µg [55]. Nunes *et al.* also investigated an electrochemical sensor made of reduced graphene oxide-Sb for detecting Cd(II) ions whose detection limit was 20.5 nM. This sensor showed a linear range between 50 and 120 nM [56]. However, as mentioned before, compared to other methods, carbon paste electrodes are less complex and low cost, making them an alternative option for other methods [8].
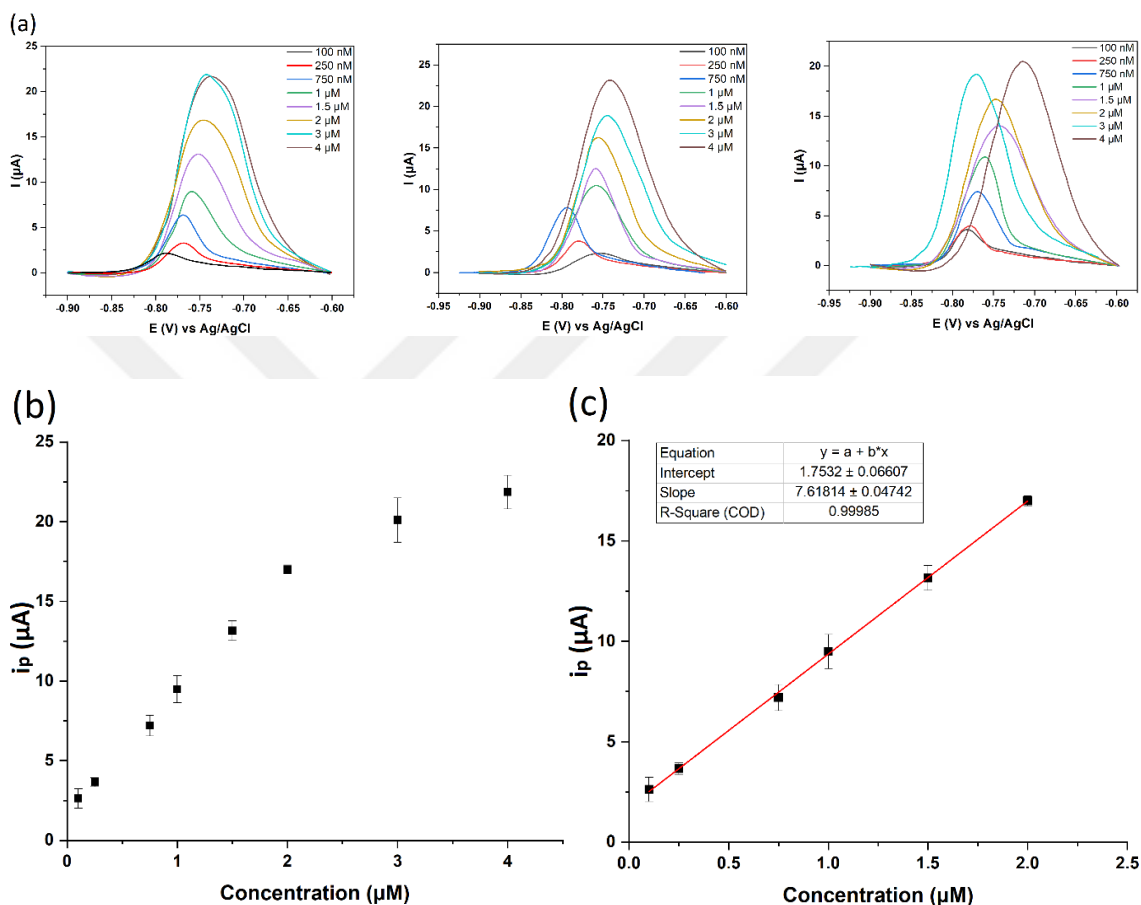
Figure 20. (a) DPASV peaks using optimum parameters for plotting the calibration curve (for each concentration, the DPASV test was repeated three times), (b) peak current vs. Cd(II) concentration, and (c) calibration curve of the *S. aureus*-modified biosensor.

3.5   Selectivity of the developed biosensor for detecting Cd(II)

The matrix effect of interfering heavy metal ions, including Cu(II), Co(II), Pb(II), Ni(II), and Zn(II), on the detection of Cd(II) ions in PBS buffer, was investigated using DPASV (Figure 21 a and b). For this purpose, optimum parameters (pH 6, preconcentration time of 15 minutes, and scan rate of 10 mV/s) were employed. The concentration of the Cd(II) in all solutions (1, 2, 3, 4, and 5) was constant and 250 nM, and there were no interfering heavy metal ions in the first solution (1). However, interfering heavy metal ions

27

concentration in solutions 2, 3, 4, and 5 was 250 nM, 500 nM, 750 nM, and 1 μM, respectively. According to Figure 21 b, the addition of interfering heavy metal ions reduced the anodic peak sharpness of Cd(II). Moreover, as the concentration of the interfering heavy metal ions was increased to 1 μM (solution 5), a small peak appeared around -0.6 V belonging to Pb(II). These results showed the competition between heavy metal ions for binding to the biosensor's surface [30].
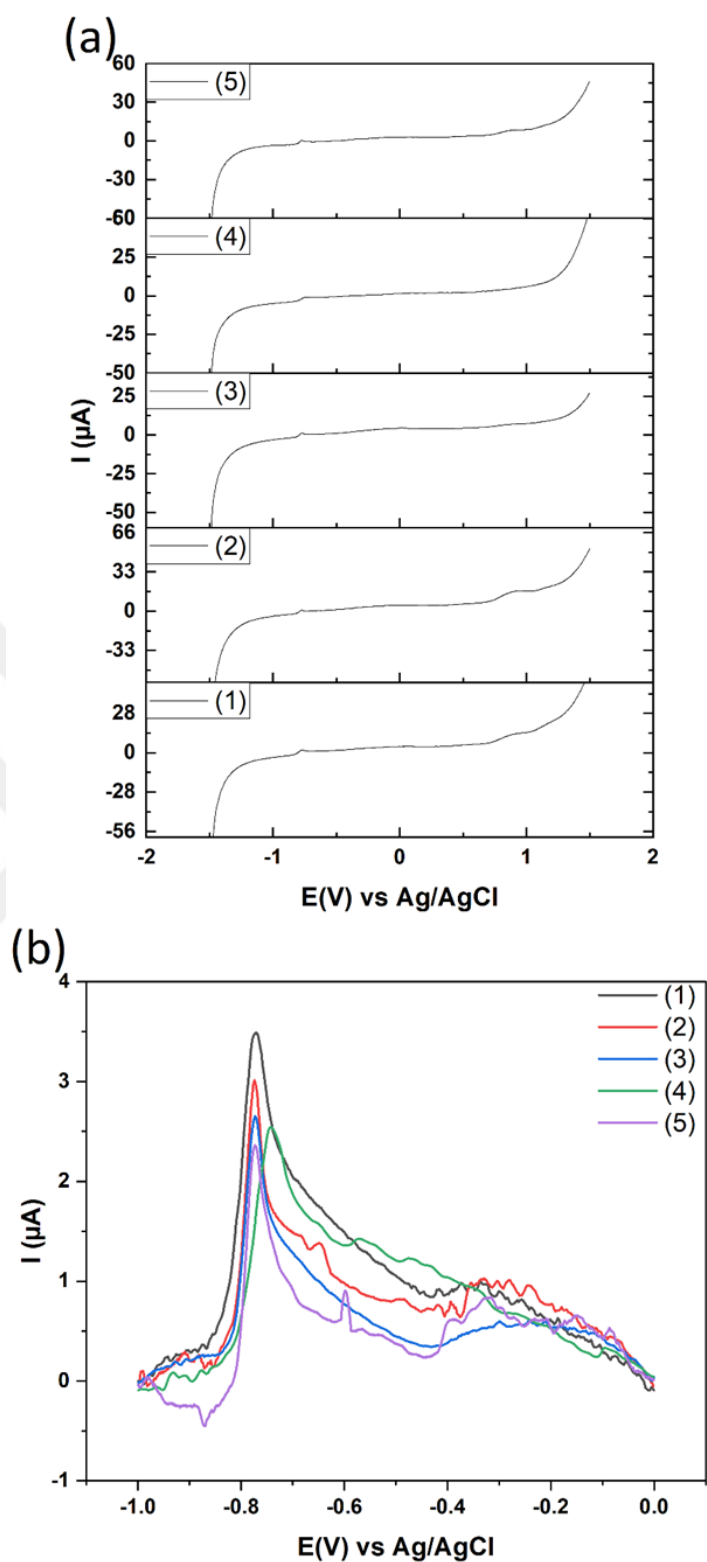
Figure 21. (a) DPASV curves, and (b) enlarged DPASV peaks obtained in PBS buffer containing (1): 250 nM Cd(II), (2): 250 nM Cd(II), and 250 nM of all interfering heavy metal ions(3): 250 nM Cd(II) and 500 nM of all interfering heavy metal ions, (4) 250 nM Cd(II) and 750 nM of all interfering heavy metal ions, (5) 250 nM Cd(II) and 1 µM of all interfering heavy metal ions.

4 CONCLUSION

The main goal of the present study was to detect Cd(II), Co(II), Cu(II), Ni(II), Pb(II), and Zn(II) ions in aqueous media using a new microbial biosensor. For this purpose, a dead *S. aureus*-modified carbon paste biosensor was developed. The reason for choosing this type of biosensor was its low cost and simple preparation. CV and DPASV measurements and SEM, EDX, and FTIR results confirmed the developed biosensor's ability to detect Cd(II) ions instead of unmodified carbon paste, which was unable to detect Cd(II) ions. Moreover, it was shown that buffer type, pH, and preconcentration time could significantly affect the biosensor's performance. According to the FTIR results, it was observed that the presence of phosphate groups plays a vital role in detecting Cd(II) ions.

Consequently, according to the obtained results, it can be concluded that this new microbial biosensor can be an inexpensive, easy to develop, and efficient alternative for other expensive, complicated methods to detect heavy metals. Therefore, this biosensor has a great potential to be investigated to determine other heavy metals in different buffers.

5 REFERENCES

[1]   R.G. R. Singh, N. Gautam, A. Mishra, Heavy metals and living systems: An overview, (2011) 246–253. https://doi.org/https://dx.doi.org/10.4103%2F0253-7613.81505.

[2]   F. Length, Heavy metal pollution and human biotoxic effects, Int. J. Phys. Sci. 2 (2007) 112–118. https://doi.org/10.5897/IJPS.9000289.

[3]   T.W. Lane, F.M.M. Morel, A biological function for cadmium in marine diatoms, Proc. Natl. Acad. Sci. U. S. A. 97 (2000) 4627–4631. https://doi.org/10.1073/pnas.090091397.

[4]   J. Chronopoulos, C. Haidouti, A. Chronopoulou-Sereli, I. Massas, Variations in plant and soil lead and cadmium content in urban parks in Athens, Greece, Sci. Total Environ. 196 (1997) 91–98. https://doi.org/10.1016/S0048-9697(96)05415-0.

[5]   L. Pujol, D. Evrard, K. Groenen-Serrano, M. Freyssinier, A. Ruffien-Cizsak, P. Gros, Electrochemical sensors and devices for heavy metals assay in water: The French groups' contribution, Front. Chem. 2 (2014) 1–24. https://doi.org/10.3389/fchem.2014.00019.

[6]   Y.H. Jin, A.B. Clark, R.J.C. Slebos, H. Al-refai, J.A. Taylor, T.A. Kunkel, M.A. Resnick, D.A. Gordenin, NIH Public Access, 34 (2009) 326–329. https://doi.org/10.1038/ng1172.Cadmium.

[7]   H.C. Dalurzo, L.M. Sandalio, M. Gómez, L.A. Del Río, Cadmium Infiltration of Detached Pea Leaves: Effect on its Activated Oxygen Metabolism, Phyt. - Ann. Rei Bot. 37 (1997) 59–64.

[8]   M. Yüce, H. Nazir, G. Dönmez, A voltammetric Rhodotorula mucilaginosa modified microbial biosensor for Cu(II) determination, Bioelectrochemistry. 79 (2010) 66–70. https://doi.org/10.1016/j.bioelechem.2009.11.003.

[9]   P. Mohanraj, S. Bhuvaneshwari, M.S. Sreelekshmi, V. Chandra Sekhar, K. Narsimhulu, B. Kiran, S. Kumar, Bio-modified carbon paste electrode for the detection of pb(II) ions in wastewater, Water Sci. Technol. 80 (2019) 2058–2066. https://doi.org/10.2166/wst.2020.045.

[10] WHO, Chemical Fact Sheets: Cadmium, World Heal. Organ. (2003) 317–319.

[11] P. Pohl, Determination of metal content in honey by atomic absorption and emission spectrometries, TrAC - Trends Anal. Chem. 28 (2009) 117–128. https://doi.org/10.1016/j.trac.2008.09.015.

[12] E.L. Silva, P. dos S. Roldan, M.F. Giné, Simultaneous preconcentration of copper, zinc, cadmium, and nickel in water samples by cloud point extraction using 4-(2-pyridylazo)-resorcinol and their determination by inductively coupled plasma optic emission spectrometry, J. Hazard. Mater. 171 (2009) 1133–1138. https://doi.org/10.1016/j.jhazmat.2009.06.127.

[13] M. Yüce, H. Nazir, G. Dönmez, An advanced investigation on a new algal sensor determining Pb(II) ions from aqueous media, Biosens. Bioelectron. 26 (2010) 321–326. https://doi.org/10.1016/j.bios.2010.08.022.

[14] J. Kudr, H.V. Nguyen, J. Gumulec, L. Nejdl, I. Blazkova, B. Ruttkay-Nedecky, D. Hynek, J. Kynicky, V. Adam, R. Kizek, Simultaneous automatic electrochemical detection of zinc, cadmium, copper and lead ions in environmental samples using a thin-film mercury electrode and an artificial neural network, Sensors (Switzerland). 15 (2015) 592–610. https://doi.org/10.3390/s150100592.

[15] Y. Lu, X. Liang, C. Niyungeko, J. Zhou, J. Xu, G. Tian, A review of the identification and detection of heavy metal ions in the environment by voltammetry, Talanta. 178 (2018) 324–338. https://doi.org/10.1016/j.talanta.2017.08.033.

[16] J.J. Silva, L.L. Paim, N.R. Stradiotto, Simultaneous determination of iron and copper in ethanol fuel using nafion/carbon nanotubes electrode, Electroanalysis. 26 (2014) 1794–1800. https://doi.org/10.1002/elan.201400136.

[17] I. Bontidean, C. Berggren, G. Johansson, E. Csöregi, B. Mattiasson, J.R. Lloyd, K.J. Jakeman, N.L. Brown, Detection of Heavy Metal Ions at Femtomolar Levels Using Protein-Based Biosensors, Anal. Chem. 70 (1998) 4162–4169. https://doi.org/10.1021/ac9803636.

[18] J. Sochor, O. Zitka, D. Hynek, E. Jilkova, L. Krejcova, L. Trnkova, V. Adam, J. Hubalek, J. Kynicky, R. Vrba, R. Kizek, Bio-sensing of cadmium(II) ions using Staphylococcus aureus, Sensors. 11 (2011) 10638–10663.

https://doi.org/10.3390/s111110638.

[19]   S. Anandhakumar, J. Mathiyarasu, K.L.N. Phani, V. Yegnaraman, Simultaneous Determination of Cadmium and Lead Using PEDOT/PSS Modified Glassy Carbon Electrode, Am. J. Anal. Chem. 02 (2011) 470–474. https://doi.org/10.4236/ajac.2011.24056.

[20]   M.B. Gumpu, S. Sethuraman, U.M. Krishnan, J.B.B. Rayappan, A review on detection of heavy metal ions in water - An electrochemical approach, Sensors Actuators, B Chem. 213 (2015) 515–533. https://doi.org/10.1016/j.snb.2015.02.122.

[21]   D. Zhao, X. Guo, T. Wang, N. Alvarez, V.N. Shanov, W.R. Heineman, Simultaneous Detection of Heavy Metals by Anodic Stripping Voltammetry Using Carbon Nanotube Thread, Electroanalysis. 26 (2014) 488–496. https://doi.org/10.1002/elan.201300511.

[22]   A. Lochab, R. Sharma, S. Kumar, R. Saxena, Recent advances in carbon based nanomaterials as electrochemical sensor for toxic metal ions in environmental applications, Mater. Today Proc. 45 (2020) 3741–3753. https://doi.org/10.1016/j.matpr.2021.01.271.

[23]   N. Promphet, P. Rattanarat, R. Rangkupan, O. Chailapakul, N. Rodthongkum, An electrochemical sensor based on graphene/polyaniline/polystyrene nanoporous fibers modified electrode for simultaneous determination of lead and cadmium, Sensors Actuators, B Chem. 207 (2015) 526–534. https://doi.org/10.1016/j.snb.2014.10.126.

[24]   M.S. FINSTEIN, Microbes and Man, Soil Sci. 155 (1993) 360. https://doi.org/10.1097/00010694-199305000-00009.

[25]   D.A. Baruahctive, D.S. C. Nath, Aavishkar Publishers , Distributors, 2013.

[26]   A. Mai-Prochnow, M. Clauson, J. Hong, A.B. Murphy, Gram positive and Gram negative bacteria differ in their sensitivity to cold plasma, Sci. Rep. 6 (2016) 1–11. https://doi.org/10.1038/srep38610.

[27]   L. Freeman-Cook, and K. Freeman-Cook, Staphylococcus aureus infections, First edit, Chelsea House Publishers, 2006.

[28] T.Y. Liu, Y. Chen, H.H. Wang, Y.L. Huang, Y.C. Chao, K.T. Tsai, W.C. Cheng, C.Y. Chuang, Y.H. Tsai, C.Y. Huang, D.W. Wang, C.H. Lin, J.K. Wang, Y.L. Wang, Differentiation of bacteria cell wall using Raman scattering enhanced by nanoparticle array, J. Nanosci. Nanotechnol. 12 (2012) 5004–5008. https://doi.org/10.1166/jnn.2012.4941.

[29] R.A. Alfadaly, A. Elsayed, R.Y.A. Hassan, A. Noureldeen, H. Darwish, A.S. Gebreil, Microbial sensing and removal of heavy metals: Bioelectrochemical detection and removal of chromium(vi) and cadmium(ii), Molecules. 26 (2021). https://doi.org/10.3390/molecules26092549.

[30] M. Yüce, H. Nazir, G. Dönmez, Using of Rhizopus arrhizus as a sensor modifying component for determination of Pb(II) in aqueous media by voltammetry, Bioresour. Technol. 101 (2010) 7551–7555. https://doi.org/10.1016/j.biortech.2010.04.099.

[31] M. Yüce, H. Nazir, G. Dönmez, Utilization of heat-dried Pseudomonas aeruginosa biomass for voltammetric determination of Pb(II), N. Biotechnol. 28 (2011) 356–361. https://doi.org/10.1016/j.nbt.2010.11.005.

[32] Ş. Alpat, S.K. Alpat, B.H. Çadirci, I. Yaşa, A. Telefoncu, A novel microbial biosensor based on Circinella sp. modified carbon paste electrode and its voltammetric application, Sensors Actuators, B Chem. 134 (2008) 175–181. https://doi.org/10.1016/j.snb.2008.04.044.

[33] Z. Aksu, S. Ertuğrul, G. Dönmez, Single and binary chromium(VI) and Remazol Black B biosorption properties of Phormidium sp., J. Hazard. Mater. 168 (2009) 310–318. https://doi.org/10.1016/j.jhazmat.2009.02.027.

[34] C. Sp, COMPARISON OF COPPER (II) BIOSORPTIVE PROPERTIES OF LIVE AND TREATED, 36 (2001) 367–381.

[35] B.E. Taştan, S. Ertuğrul, G. Dönmez, Effective bioremoval of reactive dye and heavy metals by Aspergillus versicolor, Bioresour. Technol. 101 (2010) 870–876. https://doi.org/10.1016/j.biortech.2009.08.099.

[36] A. Rizvi, B. Ahmed, A. Zaidi, M.S. Khan, Biosorption of heavy metals by dry biomass of metal tolerant bacterial biosorbents: an efficient metal clean-up strategy, Environ. Monit. Assess. 192 (2020). https://doi.org/10.1007/s10661-020-

08758-5.

[37] Y.L. Xie, S.Q. Zhao, H.L. Ye, J. Yuan, P. Song, S.Q. Hu, Graphene/CeO2 hybrid materials for the simultaneous electrochemical detection of cadmium(II), lead(II), copper(II), and mercury(II), J. Electroanal. Chem. 757 (2015) 235–242. https://doi.org/10.1016/j.jelechem.2015.09.043.

[38] P. Prabhakaran, M.A. Ashraf, W.S. Aqma, Microbial stress response to heavy metals in the environment, RSC Adv. 6 (2016) 109862–109877. https://doi.org/10.1039/c6ra10966g.

[39] L. Baldrianova, P. Agrafiotou, I. Svancara, A.D. Jannakoudakis, S. Sotiropoulos, The effect of acetate concentration, solution pH and conductivity on the anodic stripping voltammetry of lead and cadmium ions at in situ bismuth-plated carbon microelectrodes, J. Electroanal. Chem. 660 (2011) 31–36. https://doi.org/10.1016/j.jelechem.2011.05.028.

[40] Z. Koudelkova, T. Syrovy, P. Ambrozova, Z. Moravec, L. Kubac, D. Hynek, L. Richtera, V. Adam, Determination of zinc, cadmium, lead, copper and silver using a carbon paste electrode and a screen printed electrode modified with chromium(III) oxide, Sensors (Switzerland). 17 (2017). https://doi.org/10.3390/s17081832.

[41] X. Zheng, S. Chen, J. Chen, Y. Guo, J. Peng, X. Zhou, R. Lv, J. Lin, R. Lin, Highly sensitive determination of lead(II) and cadmium(II) by a large surface area mesoporous alumina modified carbon paste electrode, RSC Adv. 8 (2018) 7883–7891. https://doi.org/10.1039/c8ra00041g.

[42] J. Hu, Z. Li, C. Zhai, L. Zeng, M. Zhu, Photo-assisted simultaneous electrochemical detection of multiple heavy metal ions with a metal-free carbon black anchored graphitic carbon nitride sensor, Anal. Chim. Acta. 1183 (2021) 338951. https://doi.org/10.1016/j.aca.2021.338951.

[43] P. Diep, R. Mahadevan, A.F. Yakunin, Heavy metal removal by bioaccumulation using genetically engineered microorganisms, Front. Bioeng. Biotechnol. 6 (2018). https://doi.org/10.3389/fbioe.2018.00157.

[44] R.E. Marquis, K. Mayzel, E.L. Carstensen, Cation exchange in cell walls of gram-positive bacteria., Can. J. Microbiol. 22 (1976) 975–982.

https://doi.org/10.1139/m76-142.

[45] K.J. Thomas, C. V. Rice, Equilibrium binding behavior of magnesium to wall teichoic acid, Biochim. Biophys. Acta - Biomembr. 1848 (2015) 1981–1987. https://doi.org/10.1016/j.bbamem.2015.05.003.

[46] C. Rauch, M. Cherkaoui, S. Egan, J. Leigh, The bio-physics of condensation of divalent cations into the bacterial wall has implications for growth of Gram-positive bacteria, Biochim. Biophys. Acta - Biomembr. 1859 (2017) 282–288. https://doi.org/10.1016/j.bbamem.2016.12.002.

[47] R. Ding, Y.H. Cheong, A. Ahamed, G. Lisak, Heavy Metals Detection with Paper-Based Electrochemical Sensors, Anal. Chem. 93 (2021) 1880–1888. https://doi.org/10.1021/acs.analchem.0c04247.

[48] I.B. Silva, D.M. de Araújo, M. Vocciante, S. Ferro, C.A. Martínez-Huitle, E. V. Dos Santos, Electrochemical determination of lead using a composite sensor obtained from low-cost green materials: Graphite/cork, Appl. Sci. 11 (2021) 1–13. https://doi.org/10.3390/app11052355.

[49] A. Simpson, R.R. Pandey, C.C. Chusuei, K. Ghosh, R. Patel, A.K. Wanekaya, Fabrication characterization and potential applications of carbon nanoparticles in the detection of heavy metal ions in aqueous media, Carbon N. Y. 127 (2018) 122–130. https://doi.org/10.1016/j.carbon.2017.10.086.

[50] Y.M. Lai, X.F. Liang, S.Y. Yang, J.X. Wang, L.H. Cao, B. Dai, Raman and FTIR spectra of iron phosphate glasses containing cerium, J. Mol. Struct. 992 (2011) 84–88. https://doi.org/10.1016/j.molstruc.2011.02.049.

[51] A.A. Ahmed, S. Gypser, P. Leinweber, D. Freese, O. Kühn, Infrared spectroscopic characterization of phosphate binding at the goethite-water interface, Phys. Chem. Chem. Phys. 21 (2019) 4421–4434. https://doi.org/10.1039/c8cp07168c.

[52] R. Lee, Antibacterial mechanism of phosphates in Staphylococcus aureus, Retrosp. Theses Diss. (1993).

[53] T. Grunert, D. Jovanovic, W. Sirisarn, S. Johler, C. Weidenmaier, M. Ehling-Schulz, G. Xia, Analysis of Staphylococcus aureus wall teichoic acid glycoepitopes by Fourier Transform Infrared Spectroscopy provides novel insights

into the staphylococcal glycocode, Sci. Rep. 8 (2018) 1–9. https://doi.org/10.1038/s41598-018-20222-6.

[54] A. Umeda, Structure of Staphylococcus aureus cell wall determined by the freeze-substitution method, Nippon Saikingaku Zasshi. Japanese J. Bacteriol. 43 (1988) 961–969. https://doi.org/10.3412/jsb.43.961.

[55] A.A. Kava, C. Beardsley, J. Hofstetter, C.S. Henry, Disposable glassy carbon stencil printed electrodes for trace detection of cadmium and lead, Anal. Chim. Acta. 1103 (2020) 58–66. https://doi.org/10.1016/j.aca.2019.12.047.

[56] E.W. Nunes, M.K.L. Silva, I. Cesarino, Evaluation of a reduced graphene oxide-Sb nanoparticles electrochemical sensor for the detection of cadmium and lead in chamomile tea, Chemosensors. 8 (2020). https://doi.org/10.3390/CHEMOSENSORS8030053.

AĞIR METALLERİN SAPTANMASI İÇİN STAPHYLOCOCCUS AUREUS MODİFİYELİ YENİ BİR ELEKTROKİMYASAL BİYOSENSÖR

Parsa Pishva

Malzeme Bilimi ve Nanomuhendislik, MS Thesis, 2021

Dr. Meral Yuce

Cd sensor, Ağır metal algilama, elektrokimyasal sensor, mikrobiyal algilama, Staphylococcus aureus

Ağır metaller, canlı organizmalara düşük konsantrasyonlarda bile zarar verebilir. Bu nedenle, bu araştırmada, kurutulmuş Staphylococcus aureus ile modifiye edilmiş karbon pasta elektrotunun üç farklı tamponda, Tris-HCl, sodyum asetat, ve fosfat tamponlu salin (PBS) dahil olmak üzere pH 6 ve 7'de farklı ağır metal iyonlarını tespit etme yeteneği araştırılmıştır. Dönüşümlü voltametri (CV) kullanılarak, modifiye edilmiş biyosensörün Cd(II) iyonlarını tespit etme kapasitesi açıkça gösterilmiştir. Ayrıca, Cd(II)'yi saptamak için geliştirilen biyosensörün performansı üzerinde tampon pH'ı ve önderiştirilme süresinin etkileri de incelenmiştir. CV sonuçları, PBS'nin pH 6'daki sonuçları tepe akım (3 uA) ile sonuçlandığını belirtmiştir. Bu nedenle, bu tampon Cd(II)'yi saptamak için deneylerin geri kalanını gerçekleştirmek üzere birincil tampon olarak seçildi. Dört farklı zenginleştirme süresi arasında, hem CV hem de diferansiyel puls anodik sıyırma voltametrisi (DPASV) sonuçlarına göre en uygun süre 15 dakikadır. Modifiye karbon pastanın taramalı elektron mikroskobu (SEM), enerji dağıtıcı X-ışını spektroskopisi (EDX) ve Fourier dönüşümlü kızılötesi (FTIR) spektroskopisi sonuçları da Cd(II) iyonlarının adsorpsiyonunu doğrulamıştır. FTIR spektrumuna göre, fosfat grupları Cd(II) iyonlarının birikmesinde önemli bir rol oynamıştır. Modifiye edilmemiş karbon pasta kullanılarak gerçekleştirilen kontrol deneyi, Cd(II) iyonlarına karşı hiçbir tepki göstermemiştir. Son olarak, kalibrasyon eğrisi kullanılarak, biyosensörün duyarlılık limiti ve hassasiyeti sırasıyla 45 nM (5.4 μg/L) ve 7.61814 μA/μM olarak hesaplanmış ve lineerliği 100 nM (0.011 mg/L) ile 2 uM (0,22 mg/L) aralığındadır.